Clean Technologies and Environmental Policy
https://doi.org/10.1007/s10098-023-02463-w

ORIGINAL PAPER

Economic feasibility assessment of microgrids with renewable energy sources in Peruvian rural areas

Juan Carlos Quispe[1] · Angel E. Obispo[1] · Francisco Javier Alcantara[1]

Received: 29 September 2022 / Accepted: 2 January 2023

Abstract
Electrification of Peru's rural areas is an issue of vital importance for economic growth. However, these areas still have poor quality electricity service or operate in a stand-alone mode with high cost of energy. To address this problem, one of the most promising strategies proposes the use of renewable energy technologies through the implementation of electrical microgrids (MGs). In this context, this research develops the analysis of 37 cases of rural villages throughout Peru in order to obtain the optimal MG design and the most feasible areas for its implementation, considering the associated costs, geographic location and load characteristics. For this purpose, an optimization process is carried out using HOMER Pro software with the aim of sizing the MG with the minimum net present cost and cost of energy. Then, an iterative process is developed in MATLAB software to map cost values, renewable contribution, emissions, the energy charge and the annual savings in the utility bill. This analysis considers five scenarios base on a grid-connected MG (with sensitivity values of grid sellback price) and an off-grid MG system. The results show the geographic distribution of all the annual utility saving bill. For the grid-connected MG condition, it presents a profit in the range of $107.08 to $368.2 compared to loads connected to the grid; while for the off-grid MG condition, it presents a profit in the range of $1269 to $4976 in comparison with loads connected to a diesel generator.

✉ Juan Carlos Quispe
juancarlosqh@ieee.org

[1] Universidad Tecnológica del Perú, Lima, Peru

Published online: 12 January 2023

Graphical abstract

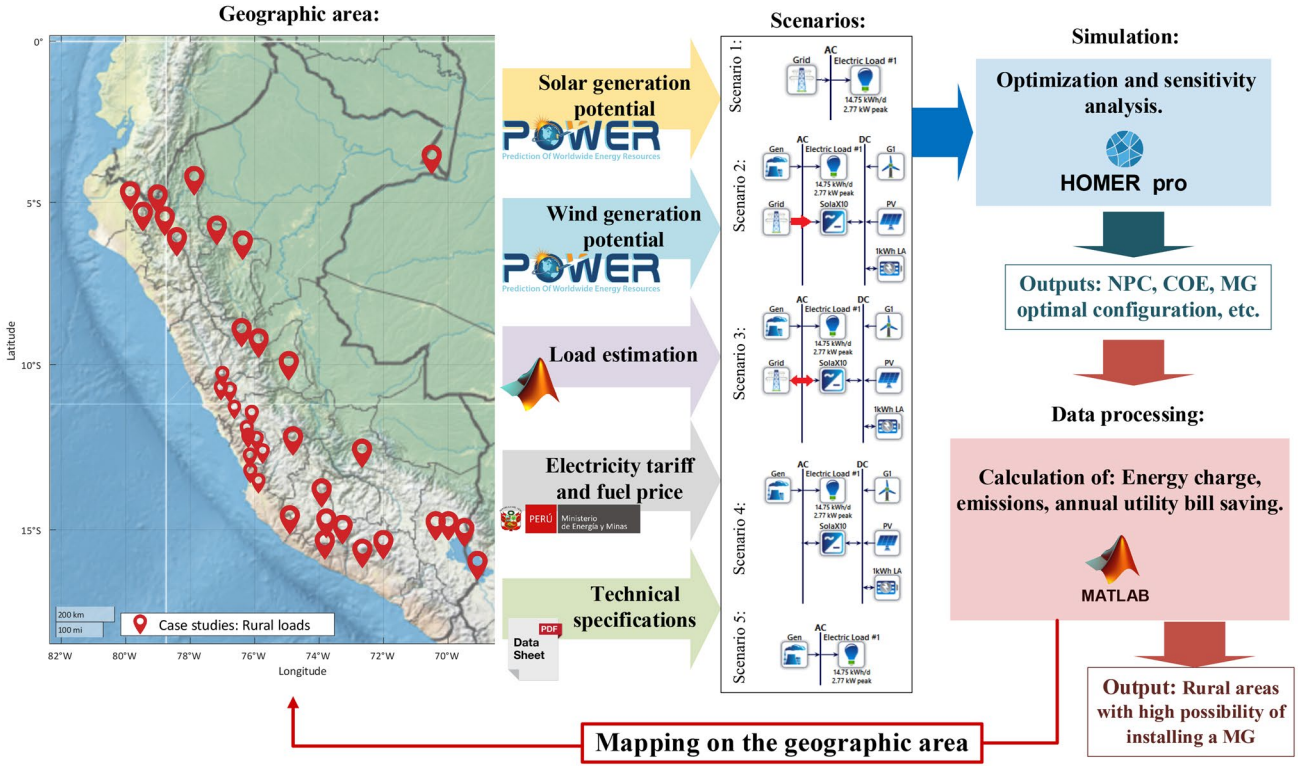

Keywords Economic · Microgrid · Optimal · Renewable energy sources · Rural area

Abbreviations

BBS	Battery bank system
CC	Capital cost
COE	Cost of energy
CRF	Capital recovery factor
DS	Diesel
EC	Energy charge
FC	Fuel cost
Homer	Hybrid optimization of multi-energy resources
INEI	National Institute of Statistics and Informatics
MG	Microgrid
NEP	Net energy purchase
NPC	Net present cost
O and MC	Operation and maintenance
PV	Photovoltaic
RC	Replacement cost
RE	Renewable energy
RES	Renewable energy source
SOC	State of charge
TNPC	Total Net present cost
WT	Wind turbine

Introduction

In recent years, electricity generation technologies based on renewable energy sources (RES) have been highlighted as an alternative way to reduce CO_2 emissions in order to address climate change. In addition, RES, unlike fossil fuels, can be harnessed at no cost to the resource. In this regard, governments have already begun to finance renewable technologies through direct subsidies, loans and tax incentives (Liu et al. 2012). Moreover, the most promising technologies are related to generation (Kroposki et al. 2020) and the use of energy storage systems (Byrne et al. 2017) due to the reduced installation cost. Therefore, the RES represents the future of the energy grid; nevertheless, this requires a smart integration and coordination system (Wang et al. 2014). It is complemented in a coordinated way with information and communication technologies by means energy management models (Arnold 2011). A representative model of this control system is the so-called electrical Microgrid (MG). The MG is defined as a set of generation sources, storage and load systems electrically connected, which are managed as a single unit, and is capable of operating both in grid-connected as well

as in stand-alone mode (Lasseter 2011; Luis Hernandez 2019). The implementation of the MGs has increased significantly, especially in rural areas, which do not have direct connection to the electrical grid, have long periods of supply interruption or poor quality of electrical service. Nevertheless, a successful implementation of this MG requires that these areas have potential for the exploitation of renewable natural resources but preserving the environment (Jha et al. 2017). In addition, certain conditions of accessibility, operability, economic and regulatory context must be taken into account, in order to have an intelligent microgrid that operates and connected to the grid or in stand-alone mode (Berizzi et al. 2019; Mojumder et al. 2022).

In order to obtain the optimal configuration of hybrid energy systems, it is necessary to use optimization tools to evaluate different scenarios. In this sense, there are optimization methods for the sizing of the system components, such as hybrid optimization of multi-energy resources (Homer 2022), particle swarm optimization, genetic algorithm (Mustafa Kamal et al. 2022; Najafi et al. 2011), cuckoo search algorithm (Ray et al. 2018), modified electric system analysis (Zahboune et al. 2016) and game theory (Khare et al. 2016). However, the application of many MG optimization algorithms is still showing weaknesses, as the available algorithms require simplifications that in many cases do not match reality, which can lead to incorrect results (a false optimum). The HOMER method has proven to be robust program capable of performing and comparing thousands of possibilities in a single run; in addition, it examines all possible combinations of user-defined equipment and cannot get "stuck" in a false optimum. In that sense, HOMER has become a reliable software as demonstrated by its wide use for research work and engineering studies.

In this regard, the potentiality for the development of MGs in some rural communities in Nigeria is researched, and it is found that the replacement to the new technologies results in the system having between 56 and 81% less net present cost (NPC) than a traditional system with diesel generator; these results were obtained through an optimization process for the sizing of the system components using HOMER (Nnaji et al. 2019). A similar analysis using HOMER was developed for rural communities in Pakistan, where a technical and economic analysis of the development of MGs is performed; in this regard, photovoltaic–wind–battery was the most viable option, and the optimal sizing of components is also obtained with $28,620 NPC, which shows 81.65% reduction in cost and 100% preserving in toxic emission (Al-Ammar et al. 2020). In addition, in the same country and different location, the most efficient option of hybrid renewable energy system is technologies such as photovoltaic, biogas and hydro turbine due to the characteristics of their economic activity (Aziz et al. 2020).

A feasibility and sensitivity analysis to explore the potentials of green energy for five locations in Bangladesh was developed with the aim of finding a hydric renewable energy source configuration; the results indicate that the total NPC is more sensitive to nominal discount rate, the grid energy price, the wind turbine lifetime, average wind speed, solar irradiance and the average electric load (Nurunnabi et al. 2019). Moreover, a feasibility analysis of MG system was carried out in a rural school in Ethiopia, and this study showed that a PV and Battery system are the best option for the conditions of the place and also highlighted the great social contribution to the community (Aemro et al. 2020). Ten localities of South African were analyzed, which determines the most feasible location to install a MG based on measurement of cost of energy, NPC, energy purchased, energy sold, energy charge, annual utility bill savings and revenue (Adefarati and Obikoya 2019).

On the other hand, some research focuses on the reduction in environmental impacts. A MG is simulated for two coastal areas of Bangladesh, and sensitivity analysis has taken place by varying the load demand; the result represented an unprecedented reduction in carbon dioxide emissions with 6666.47 kg/year (Rafi et al. 2021). A stand-alone MG in three remote islands in South Korea is modeled to control the environmental pollution caused by the use of diesel generators, and the optimization process used was HOMER (Jin et al. 2019). Moreover, a MG is implemented in Hainan, whose design allows obtaining a high economic and environmental benefit compared to the traditional model (Zhao 2020). Another study revealed that the photovoltaic–wind–diesel can reduce the CO_2 emission by 70% with respect to the diesel generators (Ajlan et al. 2017). Similar analysis was focused in Malaysia locations; it was concluded that the obtained optimal configuration of wind–diesel–battery hybrid system compared to the diesel-only system results in a lower and CO_2 emission in 2,861,113 kg/year (Hossain et al. 2017).

In addition, the development of a stand-alone MG system is analyzed, and in the pilot site of Meltemi, near the coast of Athens, the authors suggest that the installation of photovoltaic and wind turbines technologies in order to optimize its operation (Papaioannou et al. 2014). A stand-alone system situation is shown in the Province of San Luis, Argentina, where the cost of a hybrid MG and a genset is compared, and the result shows the lower total cost of the MG system with respect to the genset (Catuogno et al. 2019). Another stand-alone hybrid energy system for a village in Uttarakhand, India was studied; also, it verifies a comparison between different optimization methodologies and obtains that in all cases, there is a reduction in the total NPC of up to 7% (Mustafa Kamal et al. 2022).

In general, the best hybrid configurations for MG are made up of photovoltaic, batteries and wind turbines from a cost-effective and environmental point of view. Some works include a synchronous generator, particularly diesel, for greater operational safety. In addition, all agree that each case analyzed presents a particular behavior of the demand, discount rate, the grid energy price, solar irradiance and average wind speed, which makes it a highly variable parameter at the time of designing a MG. They also consider a local or particular analysis of a case study. This work focuses mainly on the design of MGs and considers the particular characteristics of rural areas in strategic places in Peru. Therefore, an important contribution is the analysis of the economic benefits of the implementation of MG for different geographical conditions (Coast, Andes and Amazon) and zones (North, Central and South), which have different climatic conditions; this is developed using the HOMER pro software. In addition, it includes the analysis of the typical characteristics of demand behavior for all case studies, and then, the cost-effectiveness is determined by comparing different scenarios. The scenarios studied are grid-connected MG system without grid sellback price, grid-connected MG system with grid sellback price and stand-alone MG system, and this is developed using an iterative process in MATLAB. The results show a general mapping of all the case studies, highlighting the most effective location for MG investment.

Characteristics of case studies

Thirty-seven case studies have been selected from representative sites in rural areas of Peru. The geospatial coordinates in each case as shown in Fig. 1a and Table 1. These areas are characterized by having rural electrification. Nevertheless, in most cases, these have poor quality of energy service, constant energy supply interruptions and relatively high electricity prices compared to the per capita income. In addition, in most of the cases, population has economic activities with net income around minimum salary in Peru (S/. 1025.00 = $268.71). Thus, the need arises to have a reliable and economical energy supply for these rural areas, which also have energy resources that can be exploited.

In order to identify the characteristics of the areas of Peru, certain geographical divisions are identified. From the regional point of view, Peru is divided in coast, Andes and Amazon (Fig. 1b). The coast is characterized by belonging to territories very close to the maritime coastline. The Andes are characterized by belonging to the highlands or places at high altitude above sea level. Finally, the Amazon corresponds to the tropical rainforest

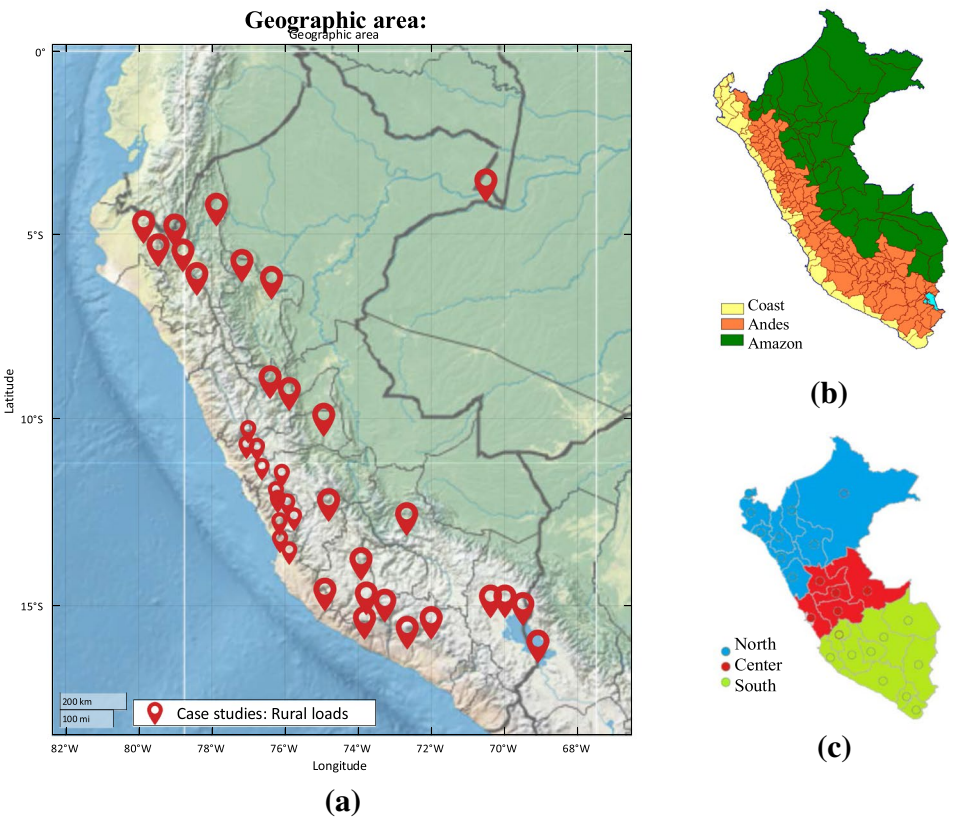

Fig. 1 Case study locations. **a** Geographical distribution of the case studies on the map of Peru, **b** regional division of Peru and **c** zonal division of Peru

Table 1 Geospatial coordinates of all case studies

Case study	Village	Geospatial	Coordinates
1	San miguel	− 10.88359	− 77.03652
2	Gracias a dios	− 6.37083	− 78.41192
3	Asquipata	− 14.10287	− 73.94447
4	Santa leonor	− 10.95934	− 76.77205
5	Hongos	− 12.81036	− 75.76516
6	Quinches	− 12.30741	− 76.14317
7	Canta	− 11.46694	− 76.62479
8	Cajatambo	− 10.47258	− 76.99296
9	Huarochiri	− 12.13673	− 76.23250
10	Huarmaca	− 5.56918	− 79.52528
11	Quicacha	− 15.62498	− 73.79810
12	Marcabamba	− 15.14982	− 73.34142
13	Humay pampano	− 13.72247	− 75.88664
14	Yauyos	− 12.45979	− 75.91856
15	Lunahuana	− 12.96574	− 76.14706
16	Coracora	− 15.01633	− 73.78358
17	Chuquibamba	− 15.83920	− 72.65147
18	Nuevo Seasme	− 4.58981	− 77.86620
19	Caballococha	− 3.91038	− 70.51621
20	Rioja Oriente	− 6.06135	− 77.16778
21	Bellavista rural	− 6.48852	− 76.36036
22	PSE Azangaro III Etapa	− 15.10665	− 69.98926
23	Rosapata	− 15.23451	− 69.52736
24	San Ignacio	− 5.14669	− 79.00501
25	Bagua-Jaen rural	− 5.68616	− 78.85348
26	Chincha rural	− 13.42520	− 76.13660
27	Nazca rural	− 14.82810	− 74.93693
28	Sector Cayumba	− 9.49446	− 75.95213
29	Valle del Mozon	− 9.27918	− 76.39625
30	Yauli, Junin	− 11.66658	− 76.08662
31	Puerto Bermudez	− 10.29790	− 74.93795
32	Tablachaca, Quichuas	− 12.47282	− 74.76742
33	Yanay	− 12.88596	− 72.64831
34	Pucara	− 15.04191	− 70.36806
35	Valle del Colca	− 15.62217	− 71.98080
36	Frontera	− 16.22721	− 69.09513
37	Santo Domingo Chalaco I y II	− 5.02975	− 79.87590

and covers most of the Amazon River basin and also includes the border with the Andes. On the other hand, from a zonal point of view, Peru is divided in north, center and south (Fig. 1c). The main characteristic of this division is the distance from the equatorial line of the earth. This characterization of the areas is very important as it allows the identification of similarities in weather conditions, economic activities and even lifestyle habits.

Solar generation potential

This information was extracted from the NASA Prediction of Worldwide Energy Resource (NASA 2022). Based on the information obtained, the southern coast and southern Andes of Peru have a high solar energy potential, while the central coast, central Andes, northern coast and northern Andes have a slightly lower but considerable solar energy potential. In contrast, the magnitude of the irradiation of the entire Amazon area has low levels. In addition, during the months of January, February, March and April, the irradiation fluctuates between 4.8 and 7 kWh/m^2/day, whereas in May, June, July and August the irradiation fluctuates between 3.8 and 6 kWh/m^2/day; also, in September, October, November and December, the irradiation ranges between 5.5 and 7.2 kWh/m^2/day. The annual average solar radiation map of Peru is presented in Fig. 2a.

Wind generation potential

Based on the climatic information from NASA Prediction of Worldwide Energy Resource (NASA 2022), the average annual wind speed in Peru is approximately 4 m/s. Moreover, during the months of July and August, the average wind speed is slightly higher compared to the rest of the year. The characteristics of wind energy in Peru are illustrated in Fig. 2b. It can be seen that there are 3 areas with wind energy higher than the rest. The south coast, the north coast and the northern Andes have areas with an annual average of more than 8 m/s.

Load estimation

The load profiles of rural areas present a typical behavior throughout the day and the year. These profiles can be categorized according to the type of users, for example, domestic users belong to the residential household in a given area. Commercial users are those that carry out some commercial activity, including activities inside households. General users correspond to schools, medical posts, churches and community centers, etc., which are part of the communal area. Finally, the users of small industry correspond, for example, to carpentry workshops, footwear, etc. This work focuses mainly on residential demands because it represents the major percentage of the demand. In addition, it has been evidenced its great importance with the latest global pandemic event, since there was a great need to have safe and reliable electricity in the users for activities associated with work, education, etc. In this sense, it is convenient to classify the localities' demand in the areas of Peru. These loads can be categorized according to the type of users described in the guide for the formulation of rural electrification projects

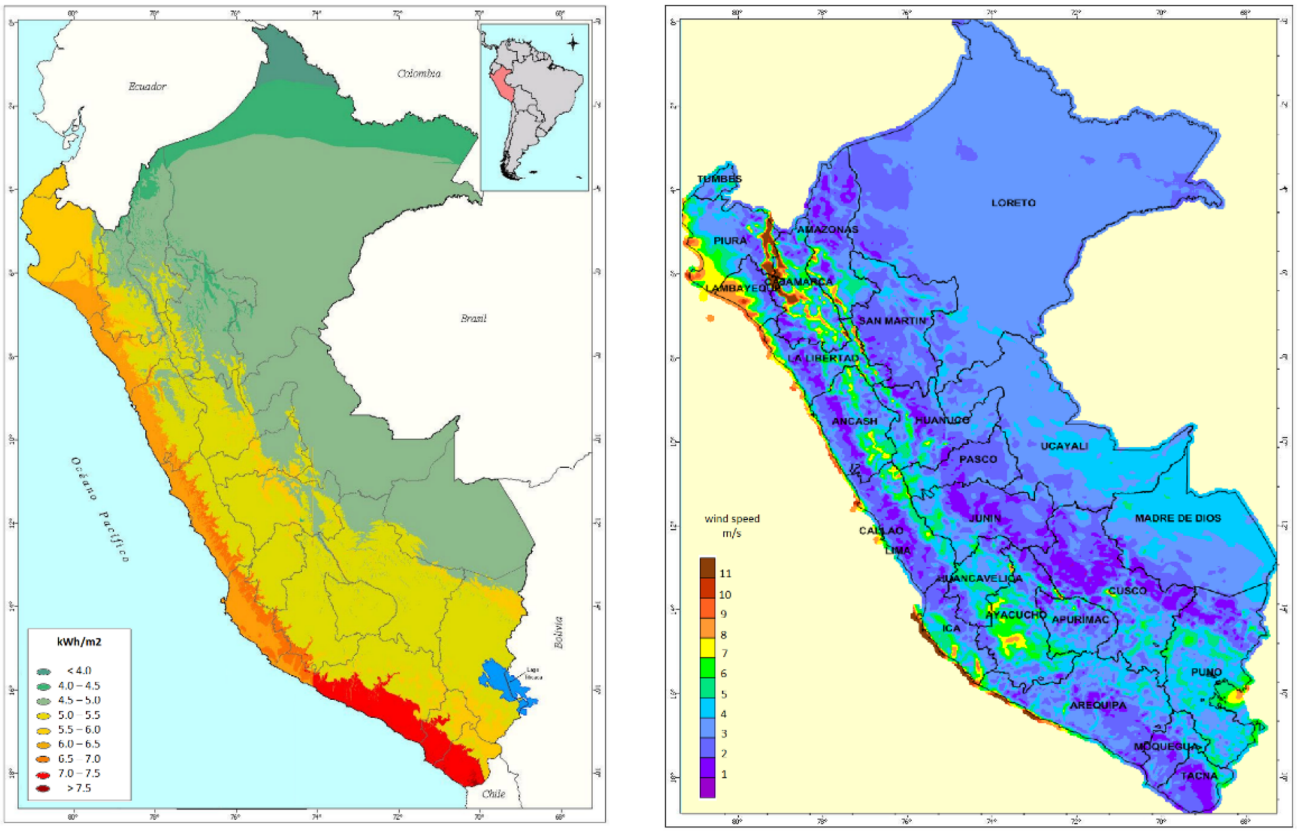

Fig. 2 Average annual of resources in Peru. **a** Solar, **b** wind

Table 2 Persons per household in rural areas

Geographic region	Person/household
Coast	4.2
Andes	3.9
Amazon	4.6

Table 3 Referential values of residential energy consumption

Geographic region	Energy consumption (kWh/month)	
	Type 1	Type 2
Coast	19–30	10–18
Andes	17–25	8–16
Amazon	20–35	12–20

developed by the Ministry of Economy and Finance (MEM 2011).

Load types

Load type 1: They are the locations concentrated or slightly dispersed within rural areas, which present a defined urban configuration and can have squares and/or streets. They also have an intermediate level of development, public services and premises and access roads.

Load type 2: They are the locations dispersed within rural areas with a smaller number of public services, stores and access roads in regular conditions (carriage trails) or without access roads.

Persons per household in rural areas

It is the result of the division between total population and number of households in rural areas. This result is based on surveys from the National Institute of Statistics and Informatics (INEI 2019). Table 2 shows the number of persons per household and per geographic region.

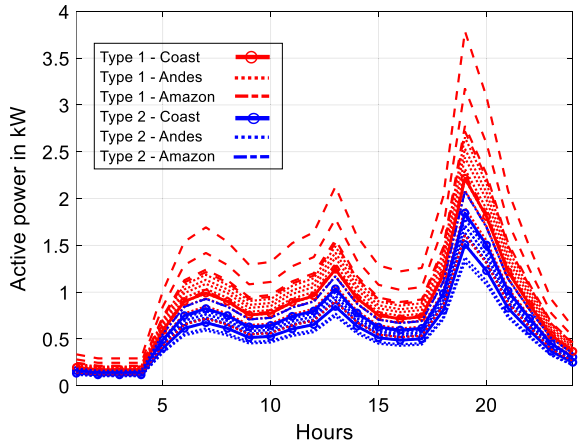

Fig. 3 Daily demand profile

Energy consumption per user

The reference energy consumption is based on the analysis of similar electrified localities and close to the study areas of the project. The likeness includes criteria such as geographical area, size of towns, level of dispersion between users, distances and access routes to the main populated center of the area and the socio-economic characteristics. This information is obtained from the utilities or companies that manage the electrical service in the area near the location. Reference values of energy consumption per domestic user in rural areas are shown in Table 3.

Daily demand profile estimation

The typical demand profiles of a residential user group in the study areas are determined based on two considerations: The typical demand profile of a residential load, provided by HOMER, and the variation of the magnitude within the

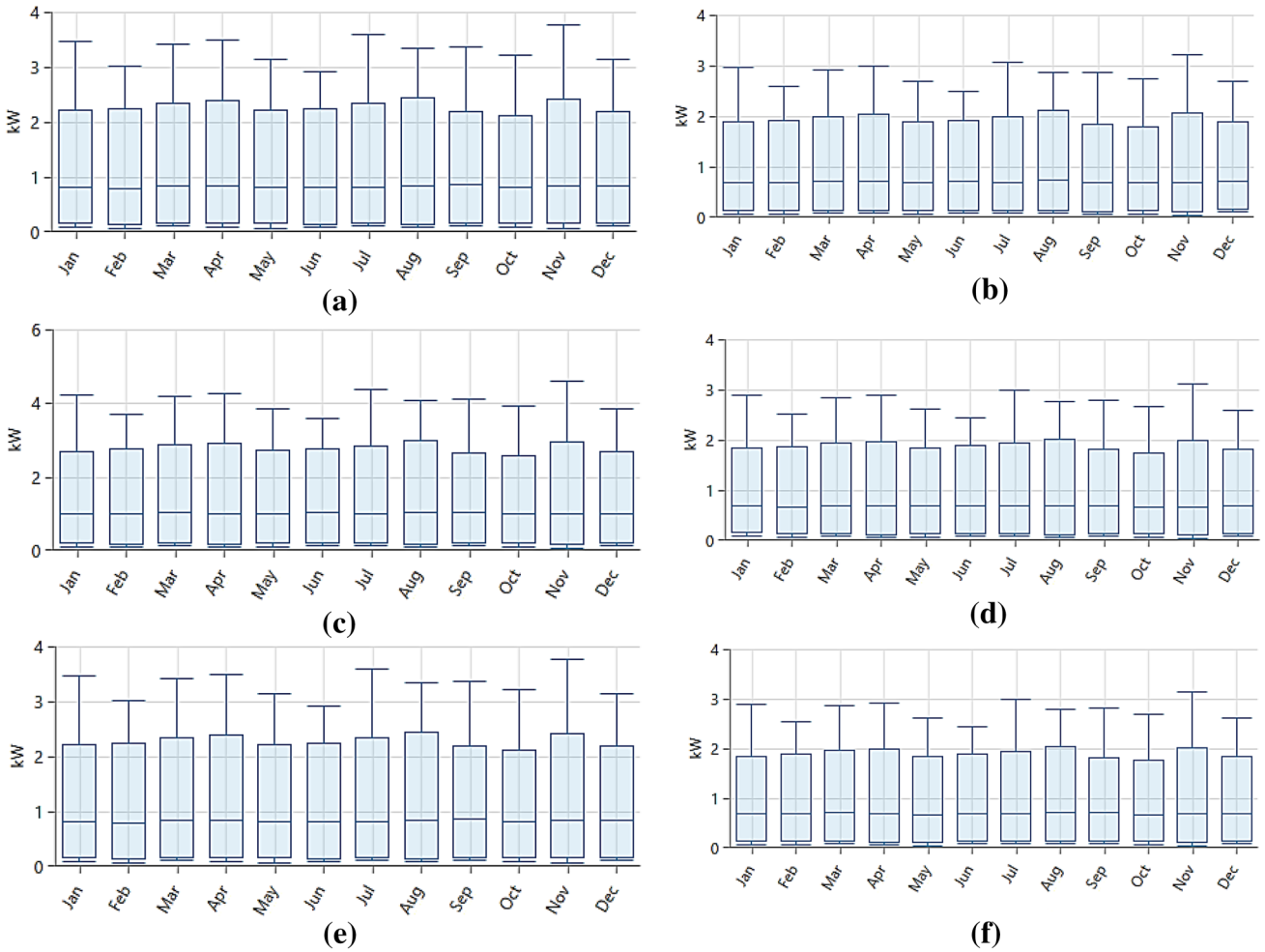

Fig. 4 Monthly average scaled demand data. **a** Type 1—Coast, **b** Type 1—Andes, **c** Type 1—Amazon, **d** Type 2—Coast, **e** Type 2—Andes and **f** Type 2—Amazon

ranges are shown in Table 3. Therefore, the hourly variation of the power magnitudes is calculated using random values determined by MATLAB functions. The result is shown in Fig. 3.

Demand profiles with season variation

Although the climatic characteristics throughout the Peruvian territory present differences due to the geographical position, topography or altitude, geographical regions, influence of marine currents, winds, influence of the El Niño phenomenon and weather conditions, variations along the seasons are not considered extreme. In this sense, the Amazon region is characterized to have a humid and tropical climate throughout the year. The Andes region is characterized to have a sub-humid and cold climate during the year, which seasonal variations of the maximum temperature are weak (Imfeld et al. 2021). The region of coast is characterized to have a desert and temperate climate. This means that the behavior of the demand does not present extreme changes with the seasonal characteristics, i.e., during the winter, the temperature is not low enough to have heating installations or during the summer, there is no need to use air conditioning since the use of fans is enough. Consequently, random behavior during the year is considered for all the case studies as shown in Fig. 4.

Energy cost of the case studies

The case studies analyzed and present a direct connection to the electrical grid; however, due to the problems mentioned above, the implementation of MGs is being evaluated with the objective of having autonomous electrical systems. The current electricity tariff for the case studies is obtained according to the tariff sheet of the utility ADINELSA (ADINELSA 2022), which has among its customers the largest number of case studies and is taken as a reference for the rest of the cases. In this context, the cost of energy of a tariff between 0 and 30 kWh has a monthly fixed charge of 2.74 S/./month (0.738 $/month) and an energy charge of 39.39 cents. S/./kWh (0.106 $/kWh). In addition, the tariff between 31 and100 kWh has a monthly fixed charge of 4.69 S/./month (1.26 $/month) and an energy charge of 79.93 cents. S/./month (0.215 $/kWh). The grid sellback price is not regulated yet in Peru, although it can be set based on the particular characteristics of each country's electrical grid (Fraunhofer 2021; Gabr et al. 2021). For the purpose of this work, the price is considered as 30% of the grid power, i.e., 0.031 $/kWh.

Table 4 PV panels specifications

PV characteristic	Generic flat plate PV	Astronergy PV
Rated capacity (kW)	0.5	0.3
Capital cost ($)	250	220
Replacement cost ($)	200	190
O and M cost ($/year)	25	22
Lifetime (years)	20	20
Derating factor (%)	80	80

Table 5 WT specifications

WT characteristic	Generic WT	Aeolos WT
Rated capacity (kW)	1	3
Capital cost ($)	1300	7000
Replacement cost ($)	1100	6000
O and M cost ($/year)	130	600
Hub height (m)	10	12
Efficiency (%)	80	80

MG components

An MG system can present different topologies and designs of generation technologies such as solar, wind, battery bank and fossil fuel-based generation, among others. In this regard, the possible components of the MG are described below.

Solar PV system

A photovoltaic cell is a semiconductor material that converts light energy into electricityand that can be installed quickly with low operating and maintenance costs. Therefore, the selection of the PV system should be based on the availability of solar radiation at a particular site, weather conditions, cell temperature, clouds, snow, shading effects and rated efficiency, etc. The total energy generated by the solar photovoltaic system (E_{SPV}) is expressed by Eq. (1).

$$E_{SPV}(t) = \frac{P_{PV} \cdot G(t) \cdot \left[1 + K_T\left(T_C - 25\right)\right] \cdot \Delta t}{G_{ref}} \quad (1)$$

where P_{PV} is the rated power of the PV system, $G(t)$ is the solar irradiance in W/m^2, G_{ref} is the solar irradiance at standard test conditions that takes the value of 1000 W/m^2, K_T is the coefficient of temperature of the solar modules, the time interval Δt is 15 min, and T_C is the cell temperature (Homer 2022; Islam et al. 2018). The input data of the PV panels used in the MGs are listed in Table 4.

Wind turbine (WT) system

A wind turbine converts the kinetic energy of wind into electrical energy. It is a turbomachine engine that turns a rotor. The mechanical energy of the rotor shaft can be harnessed for the generation of electrical energy by means of electrical generators. The total energy generated by wind turbine system (E_{SWT}) is expressed by Eq. (2).

$$E_{SWT}(t) = 0,5 \cdot \rho \cdot C_P \cdot \pi \cdot R^2 \cdot v(t)^3 \cdot \Delta t \quad (2)$$

where $v(t)$ is the mean wind velocity at the time interval Δt, R is the blade radius, C_P is efficiency coefficient of the turbine, and ρ is the air density (Homer 2022; Ozerdem et al. 2006). The input data of the WT used in the MGs are listed in Table 5.

Battery bank system (BBS)

Solar and wind resources are essential because they have the capacity to generate clean and renewable energy. However, it is important to note that solar resources are only available during the day, whereas wind resources have a highly variable behavior. Therefore, the integration of a battery system can help mitigate these intermittent drawbacks characteristic of renewable energies. On the other hand, the BBS is usually integrated to an off-grid MG to guarantee energy supply without depending on the energy production of the MG generator at night or in time intervals when the energy resource is scarce. There are many different types of batteries on the market for renewable energy projects, but the selection of the best battery storage system depends on factors such as depth of discharge, charging efficiency, discharging efficiency, operating temperature, self-discharge, cost per kWh and charging time (Homer 2022; Kumar et al. 2018).

$$\mathrm{SOC}(t) = \mathrm{SOC}(t-1) \cdot (1-\sigma) - \frac{I_{batt} \cdot \eta_{ch}^{k} \cdot \Delta t}{C_b} \quad (3)$$

where SOC is the state of charge, σ is the self-discharging of the battery, η_{ch} is the charging efficiency, Δt is the simulation time, C_b is the nominal capacity of the battery, k takes the value of 1 when charging and zero when discharging, and I_{batt} is the charging and discharging current.

$$E_{batt}(t) = V_{batt} \cdot C_{batt}(\mathrm{SOC}(t) - \mathrm{SOC}(t-1)) \quad (4)$$

where V_{batt} is the nominal voltage of the battery, and C_{batt} is the nominal capacity.

$$I_{batt} = \frac{P_L}{\eta_{inv} \cdot V_{batt}} - I_{generation} \quad (5)$$

where P_L is the demand power of the load, and η_{inv} is the inverter efficiency. The input data of the BBS used in the MGs are listed in Table 6. Regarding battery characteristics, lead–acid batteries have the lowest investment cost per kWh, which is about 300 ($/kWh), but they have a shorter lifespan and require regular maintenance to keep them running properly. While lithium-ion batteries have a higher efficiency reaching up to 97%, and at the same time, they have a high depth of discharge ranging from 90 to 95%, but they have a cost of around $1200 ($/kWh), which is considered high compared to other technologies. Although both technologies have their advantages and disadvantages, they can easily be included in the analysis of the Microgrid design. In this work, the cheapest technology was considered as the entry cost; however, the analysis can be extended to more technologies.

Table 6 BBS specifications

BBS characteristic	Generic 1 kWh lithium-ion	Generic 1 kWh lead–acid
Nominal voltage (V)	6	12
Nominal capacity	166.6 Ah	1 kWh
Capital cost ($)	1200	300
Replacement cost ($)	1000	200
O and M cost ($/year)	20	10
Lifetime (years)	15	10
String size	1	2

Table 7 Converter specifications

Converter characteristic	Generic converter	SolaX10
Capital cost ($/kW)	300	150
Replacement cost ($)	–	–
O and M cost ($/year)	–	–
Lifetime (years)	25	25
Efficiency (%)	95	97

Table 8 Diesel specifications

Diesel characteristic	Generic diesel	Autosize genset
Capital cost ($/kW)	500	700
Replacement cost ($)	400	500
O and M cost ($/kW/h)	0.03	0.03
Lifetime (h)	15,000	15,000
Fuel price ($/L)	1.18	1.57

Bidirectional converter system

The converter system is used for exchanging power between AC and DC buses. In that sense, the inverters have as main function to convert the types of energy in Direct Current (solar generators, wind and battery bank system) to Alternating Current (Electric Grid, wind and diesel generator). The size of this converter is based on the minimum and maximum converted energy levels. The input data of the converter used in the MGs are listed in Table 7.

Diesel generator

A diesel generator is a machine that drives an electric generator through an internal combustion engine. They are generally used when there is a deficit in the generation of electricity in some area, or when there are frequent power outages. The diesel generator model is given by Eq. (6).

$$C_{\mathrm{DG}} = \alpha \cdot P_{\mathrm{DG}} + \beta \cdot P_{\mathrm{DGrated}} \tag{6}$$

where C_{DG} is the consumption of fuel (L/h), P_{DG} is the output power of the Diesel generator (kW), P_{DGrated} is the nominal power of the diesel generator (kW), and α and β are coefficients of the fuel consumption curve (in L/kWh). The input data of the diesel used in the MGs are listed in Table 8.

Methods

The process starts with the optimization problem formulation, which involves identifying the objective function and the constraints.

Total net present cost (TNPC)

It consists of the following costs: capital, replacement, operation and maintenance and fuel costs, as shown in Eq. (7).

$$\mathrm{TNPC} = \mathrm{CC} + \mathrm{O\&MC} + \mathrm{RC} + \mathrm{FC} \tag{7}$$

where CC is the total capital cost, O and MC are the total operating and maintenance cost, RC is the total replacement cost, and FC is the total fuel cost. In each case, the partial cost is the sum of the cost of each component multiplied by the number of components.

Cost of energy (COE)

It is the average cost per kWh of useful electrical energy produced by the system. It is determined using Eq. (8), as defined in (Suresh et al. 2017).

$$\mathrm{COE} = \frac{\mathrm{TNPC} \times \mathrm{CRF}}{E_{\mathrm{gen}}} \tag{8}$$

where CRF is the capital recovery factor; E_{gen} is the total energy generated by both the grid and the microgrid generators.

$$E_{\mathrm{gen}} = E_{\mathrm{gen\_load}} + E_{\mathrm{gen\_grid}} \tag{9}$$

In the case of a completely stand-alone MG system, the $E_{\mathrm{gen\_grid}} = 0$. In addition, the CRF is determined by Eq. (10).

$$\mathrm{CRF} = \frac{\gamma(1+\gamma)^{\tau}}{\gamma(1+\gamma)^{\tau} - 1} \tag{10}$$

where γ is the annual interest rate, and τ is the useful life of the plant in years.

Net energy purchase

Net energy purchase (NEP) is equal to energy purchase of energy from the grid minus the sale of energy to the grid by users. In a situation where users, in a specified period, sell more energy to the grid than they buy, a negative grid NEP is obtained. The net energy purchased is estimated by Eq. (11).

$$\mathrm{NEP}_{\mathrm{kwh}} = \left(\sum_{i=1}^{n} E_{\mathrm{purch},i} - \sum_{i=1}^{n} E_{\mathrm{sold},i} \right) \tag{11}$$

where $\mathrm{NEP}_{\mathrm{kwh}}$ is the net energy purchased (kWh) in one month, $E_{\mathrm{purch},i}$ is the energy purchased in the month i (kWh), $E_{\mathrm{sold},i}$ is the energy sold the month i (kWh), and n is the number of months.

Energy charge

The value of the energy charge by users is estimated by Eq. (12).

$$E_{\mathrm{charge}} = \left(\sum_{k}^{\mathrm{rate}} \sum_{i=1}^{n} E_{\mathrm{purch},i} \times C_{\mathrm{purch},k} - \sum_{k}^{\mathrm{rate}} \sum_{i=1}^{n} E_{\mathrm{sold},i} \times C_{\mathrm{sold},k} \right) \tag{12}$$

where E_{charge} is the energy charge (\$), $C_{\mathrm{purch},k}$ is the cost of energy purchased from the grid in month i with tariff k in \$/kWh, and $C_{\mathrm{sold},k}$ is the cost of energy sold to the grid in month i at the applied tariff k, \$/kWh.

Annual savings on electric utility bills

Annual electric utility bill savings are the difference between the actual utility bill without using renewable energy technologies and the cost of electricity with the use of renewable energy sources through MG.

$$U_{\text{savings}} = \left\{ \left(\sum_{k}^{\text{rate}} \sum_{i=1}^{n} E_{\text{grid},i} \times C_{\text{grid},k} \right) - \left(\sum_{k}^{\text{rate}} \sum_{i=1}^{n} E_{\text{purch},i} \times C_{\text{purch},k} - \sum_{k}^{\text{rate}} \sum_{i=1}^{n} E_{\text{sold},i} \times C_{\text{sold},k} \right) \right\} \tag{13}$$

where $C_{\text{grid},k}$ is the charge for energy by the electric utility without the application of the MG system, and $E_{\text{grid},i}$ is the purchase of energy from the grid without the application of MG.

Revenue

The system revenue of an MG is defined as the financial gain resulting from selling excess energy into the grid, based on the retail price of electricity and the actual cost of electricity, i.e., the production COE of the MG. This is shown in Eq. (14).

$$R_i = \sum_{k}^{\text{rate}} \sum_{i=1}^{n} E_{\text{sold},i} \times C_{\text{sold},k} - \sum_{k}^{\text{rate}} \sum_{i=1}^{n} E_{\text{sold},i} \times \text{COE}_{\text{sold},k} \tag{14}$$

where $\text{COE}_{\text{sold},k}$ is the production COE of the MG system.

Optimization process

For the development of resources optimization simulations of an MG, the specialized software HOMER Pro is used, which is an application tool produced by the National Renewable Energy Laboratory to perform techno-economic feasibility study, sensitivity analysis and optimization (Homer 2022). The optimization algorithm simulates all of the feasible system configurations defined by the search space, and it provides optimal grid systems considering an objective function and constraints. In addition, a summary of all possible arrangements organized by the NPC and the COE are shown.

Objective function

The objective function is based on minimizing the total net present cost (TNPC) referred to in Eq. (7).

Constraints

The power balance and charge or discharge battery constraints are represented in Eq. (15).

$$\sum_{j=1}^{N} P_{\text{WT}} + P_{\text{PV}} + P_{\text{diesel}} \pm P_{\text{BBS}} - P_{\text{load}} = 0 \tag{15}$$

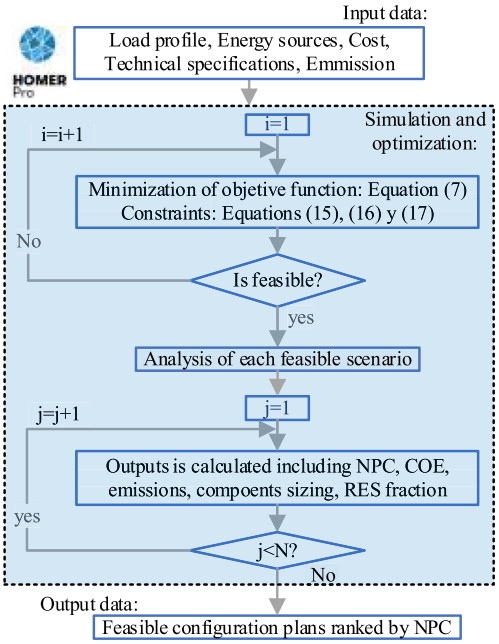

Fig. 5 Simulation and optimization procedure

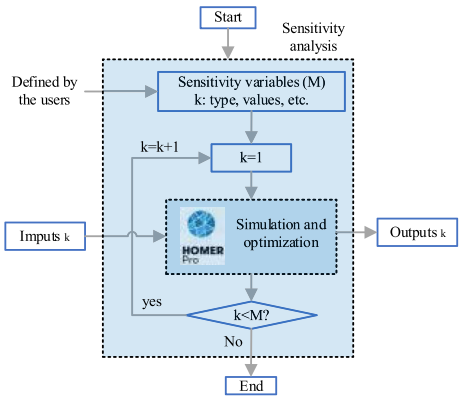

Fig. 6 Sensitivity procedure

where P_{WT} is the wind turbine power, P_{PV} corresponds to the PV generator power, and P_{BBS} is the battery system power. If P_{BBS} is positive, the battery is discharging, and P_{BBS} is negative during the charging mode.

Regarding the battery storage constraint, it is expressed in the states of charge by Eq. (16).

$$P_{\text{BBS, charge}} \leq P_{\text{BBS}}(t) \leq P_{\text{BBS, discharge}} \tag{16}$$

where $P_{\text{BBS, charge}}$ and $P_{\text{BBS, discharge}}$ represents the maximum charge and discharge of the battery system.

The lower and upper limit constraint for the solar, wind and battery systems is expressed as Eq. (17).

$$
\begin{aligned}
N_{\mathrm{WT}} &= \mathrm{Integer}, 0 \le N_{\mathrm{WT}} \le N_{\mathrm{WT}}^{\max} \\
N_{\mathrm{PV}} &= \mathrm{Integer}, 0 \le N_{\mathrm{PV}} \le N_{\mathrm{PV}}^{\max} \\
N_{\mathrm{BBS}} &= \mathrm{Integer}, 0 \le N_{\mathrm{BBS}} \le N_{\mathrm{BBS}}^{\max}
\end{aligned} \tag{17}
$$

where $N_X^{\max}$ represents the maximum number of the "X" component, which can be: wind turbines (WT), photovoltaic (PV) modules or batteries (BBS).

Simulation analysis

The operation of a MG system is simulated using hourly energy balance estimates for each year. Therefore, the evaluation is carried out considering the following factors: operation and maintenance costs, cost of capital, interest rate, inflation rate and replacement cost, among others. In addition, the inputs to the simulator are: hourly load distribution, renewable resources, energy cost, storage system, generation technical specifications and AC/DC converter technical specifications. The HOMER Pro software outputs a list of feasible configurations based on the users' specified search space. It uses a unique derivative-free algorithm to rank based on the NPC ordered from lowest to highest. The simulation and optimization procedure are shown in Fig. 5.

Sensitivity analysis

Sensitivity analysis can support the designer in evaluating the effectiveness of certain input parameters on the performance, feasibility, robustness and economy of a specific system configuration. This is an optional step that allows

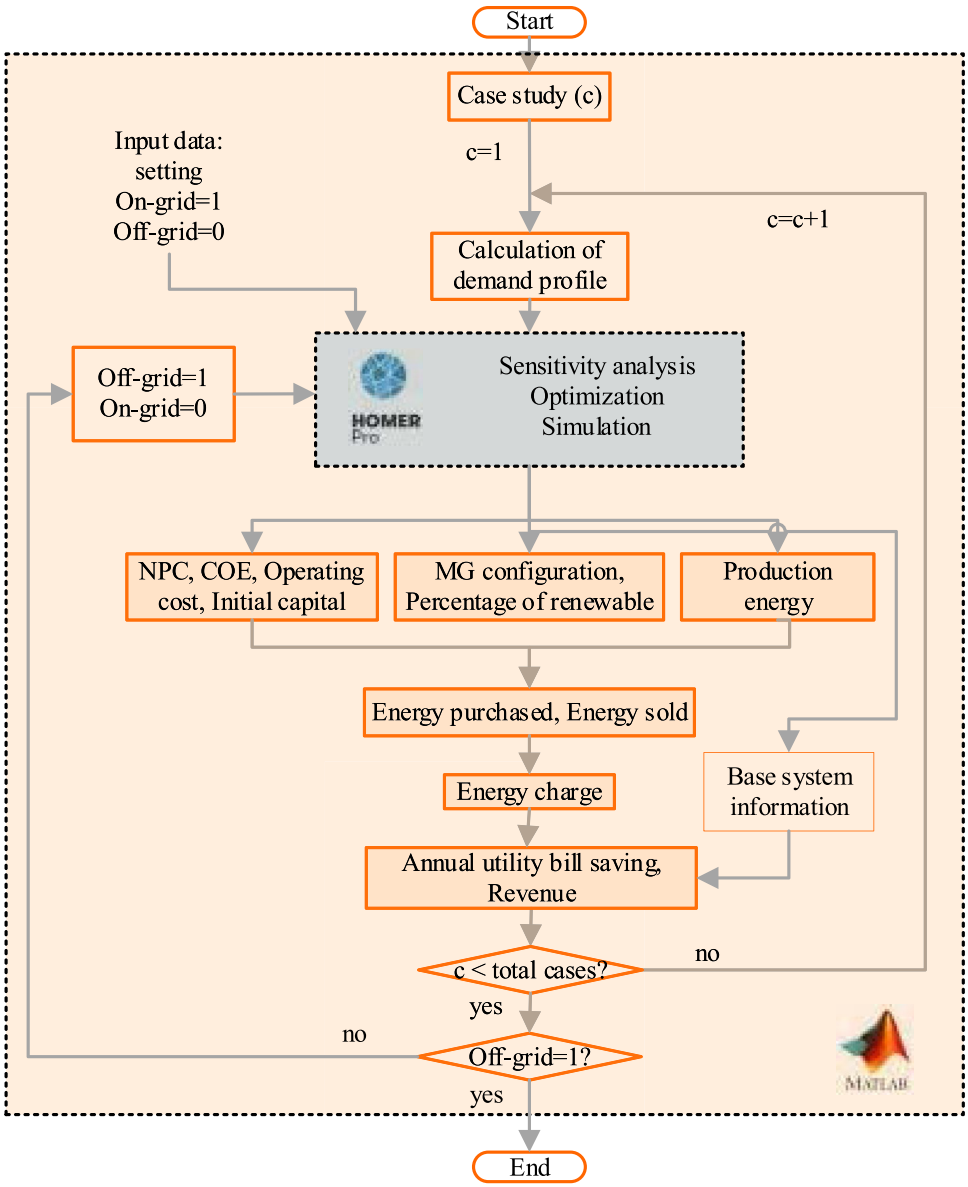

Fig. 7 Economic analysis procedure for all cases

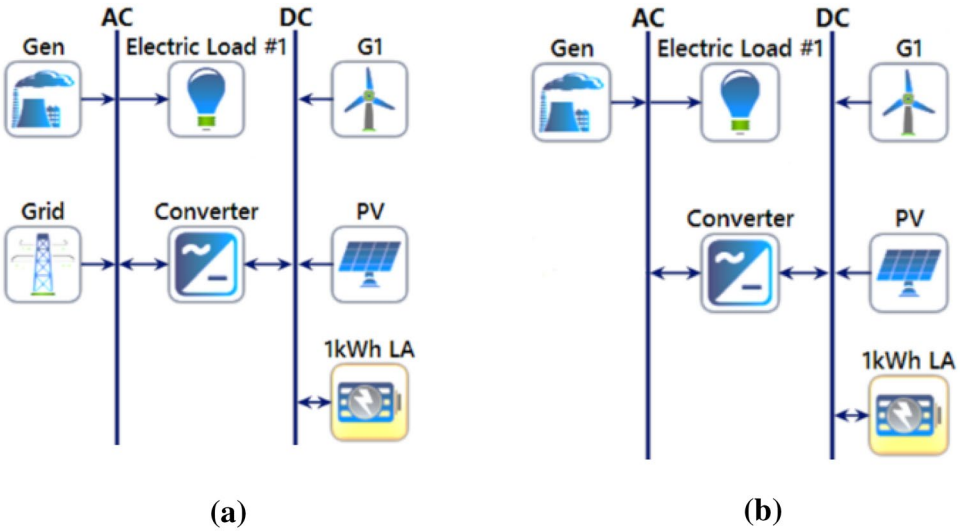

Fig. 8 MG configuration. **a** Grid-connected, **b** stand-alone

you to model the impact of variables that are beyond your control and see how the optimal system changes with these variations. The optimization procedure is repeated for each sensitivity variable (see Fig. 6), and it shows the characteristics of the results as a function of the specified input data values (Sinha and Chandel 2015).

Methodology

From the data obtained above, the energy production and energy cost are extracted; then, the energy charge for each case in grid-connected (on-grid) and off-grid system is determined. The same analysis is carried out considering grid sellback price as a sensitivity variable. Therefore, the economic benefit for each scenario is developed by comparing with the base system, which consists of a system supplied only by the grid and a system supplied only by a diesel generator. This process is shown in Fig. 7, and the following scenarios are considered:

- Scenario 1: Demand only grid-connected.
- Scenario 2: MG grid-connected without grid sellback price.
- Scenario 3: MG grid-connected with grid sellback price.
- Scenario 4: Off-grid MG system.
- Scenario 5: Off-grid load only with diesel generator.

Results and discussion

In this section, the results of the 37 case studies are discussed. Grid-connected systems (Fig. 8a) and stand-alone systems (Fig. 8b) are the study scenarios to supply the demand. The components of the MGs are: the electrical grid (in the case of the grid-connected MG), photovoltaic generator, wind turbine, battery bank system, converter and diesel generator. Moreover, a sensitivity analysis has been performed considering the grid sellback price.

- The lifetime of the proposed microgrid system is assumed to be 25 years.
- The interest rate is assumed to be 8%.
- The inflation rate is assumed to be 2%.
- The average solar resources of the selected locations are based on the NASA meteorology and solar energy databank.
- The same components of the microgrid system are used for all the locations.

According to the simulations of all case studies, the NPC values for all configurations are extracted. Table 9 shows the results of the main hybrid system configurations. The grid-connected mode are: PV-Grid, PV–BBS-Grid, PV–WT-Grid and PV–BBS–WT-Grid (Scenario 2), and the optimal configuration in off-grid mode is: PV–BBS–DS (Scenario 4). In addition, this shows the variation of the power supplied mainly by PV for all the cases of study in the grid-connected MG system. On the other hand, for the off-grid system (PV–BBS–DS column), the variation of the capacity is presented in all its components. It is also verified that the absence of the grid causes high costs in the use of batteries followed by the diesel generator.

Figure 9 shows the hybrid MG system configurations in order of priority from low to high NPC value. It is observed that all cases present the PV-grid configuration as the most cost-effective, while in second place is the PV–BBS-grid configuration for case studies: 1, 3–9, 11–23 and 25–36, in

Table 9 Results of NPC ($) for main configurations of the hybrid systems

Cases	PV-Grid		PV–BBS-Grid			PV–WT-Grid			PV–BBS–WT-Grid					PV–BBS–DS		
	NPC ($)	PV (kW)	NPC ($)	PV (kW)	BBS (1kWh)	NPC ($)	PV (kW)	TW	NPC ($)	PV (kW)	TW	BBS (1kWh)	NPC ($)	PV (kW)	BBS (1kWh)	DS (kW)
1	**4837.3**	1.383	**5006.7**	1.611	2	**6025.2**	1.376	1.00	**6381.4**	1.563	1.00	2	**11,719.2**	6.242	20	3.10
2	**6340.1**	1.850	**6527.3**	2.048	2	**6527.3**	1.781	1.00	**7806.3**	1.979	1.00	2	**16,242.8**	10.714	26	3.90
3	**4640.3**	1.348	**4717.9**	1.408	2	**5828.3**	1.292	1.00	**6161.1**	1.325	1.00	2	**9027.0**	6.516	38	0.00
4	**5042.2**	1.475	**5203.6**	1.646	2	**6268.5**	1.462	1.00	**6634.7**	1.650	1.00	2	**11,941.1**	7.125	22	3.20
5	**4012**	1.158	**4173.1**	1.376	2	**5008.3**	1.144	1.00	**5571.5**	1.354	1.00	2	**9243.9**	5.678	16	2.60
6	**5685.5**	1.621	**5859.5**	1.822	2	**7065.1**	1.580	1.00	**7224.5**	1.773	1.00	2	**14,276.5**	8.109	24	3.60
7	**6144.8**	1.799	**6298.3**	1.979	2	**7639.3**	1.798	1.00	**7719**	1.979	1.00	2	**15,023.6**	7.856	26	3.90
8	**7861.4**	2.262	**8011.3**	2.400	2	**8669.6**	2.247	1.00	**9409.9**	2.392	1.00	2	**19,666.6**	11.575	32	5.00
9	**6634.1**	1.862	**6806.7**	2.098	2	**7484.5**	1.833	1.00	**8172.3**	1.865	1.00	2	**17,583.7**	9.390	28	4.20
10	**8216.3**	2.356	**8386.3**	2.567	2	**8289.3**	1.700	1.00	**9743.9**	2.341	1.00	2	**21,232.3**	11.818	34	5.10
11	**5346.1**	1.547	**5488.8**	1.700	2	**6687.3**	1.524	1.00	**6907.2**	1.700	1.00	2	**12,513.9**	6.472	22	3.50
12	**6716**	1.938	**6851.6**	2.154	2	**7569.4**	1.915	1.00	**8265.3**	2.147	1.00	2	**15,747.8**	8.242	28	4.40
13	**6541.6**	1.884	**6694**	2.100	2	**7327.9**	1.815	1.00	**7933.9**	1.969	1.00	2	**16,086.3**	8.928	26	4.20
14	**5231.1**	1.512	**5386.7**	1.700	2	**6534**	1.509	1.00	**6780.9**	1.700	1.00	2	**12,802.5**	7.070	22	3.40
15	**4530.6**	1.269	**4714.2**	1.491	2	**5642**	1.248	1.00	**5905.4**	1.400	1.00	2	**12,036.2**	6.827	18	2.90
16	**7345.9**	2.123	**7478.3**	2.300	2	**8142.6**	2.070	1.00	**8822.9**	2.335	1.00	2	**17,227.5**	9.663	30	4.80
17	**7028.2**	2.017	**7158.3**	2.156	2	**7888.5**	2.012	1.00	**8604.7**	2.156	1.00	2	**16,383.1**	8.438	30	4.60
18	**5934.2**	1.596	**6197.4**	1.838	2	**7033.7**	1.594	1.00	**7519.2**	1.797	1.00	2	**18,187.4**	11.499	24	3.40
19	**12,067**	3.339	**12,282**	3.609	2	**12,980**	3.336	1.00	**13,669**	3.500	1.00	2	**35,255.0**	21.538	50	7.10
20	**10,092**	2.798	**10,307**	3.062	2	**10,954**	2.723	1.00	**11,586**	3.021	1.00	2	**29,510.5**	18.719	42	6.00
21	**7311.7**	1.988	**7561.2**	2.314	2	**8214.6**	1.969	1.00	**8892**	2.275	1.00	2	**22,260.1**	13.854	32	4.30
22	**4383.9**	1.250	**4531.4**	1.433	2	**5180.6**	1.196	1.00	**5793.8**	1.377	1.00	2	**10,274.3**	5.441	18	2.90
23	**3834.3**	1.090	**3985.3**	1.313	2	**4792.3**	1.038	1.00	**5247.6**	1.250	1.00	2	**8965.7**	4.472	16	2.50
24	**8387.9**	2.438	**8557.8**	2.629	2	**8482.9**	2.366	1.00	**9832.3**	2.553	1.00	2	**21,660.1**	12.307	34	5.20
25	**5760.1**	1.578	**5998.8**	1.799	2	**6525.7**	1.417	1.00	**7076.7**	1.700	1.00	2	**16,987.6**	10.819	24	3.40
26	**8591**	2.389	**8743.1**	2.514	2	**9304.7**	2.272	1.00	**9890.3**	2.447	1.00	2	**22,507.7**	11.222	36	5.50
27	**5465.3**	1.577	**5603.4**	1.781	2	**6845**	1.550	1.00	**6993.6**	1.743	1.00	2	**12,713.2**	6.713	22	3.60
28	**5938.6**	1.644	**6178.1**	1.924	2	**7279.8**	1.640	1.00	**7527**	1.843	1.00	2	**17,825.9**	11.167	24	3.50
29	**5698.1**	1.619	**5893.2**	1.836	2	**7039.3**	1.596	1.00	**7272.9**	1.723	1.00	2	**15,596.7**	9.101	22	3.50
30	**2786.8**	0.788	**2977.2**	1.034	2	**3476.6**	0.756	1.00	**4306.4**	0.938	1.00	2	**7160.6**	3.473	12	1.80
31	**11,796**	3.183	**12,275**	3.200	2	**12,841**	3.197	1.00	**13,378**	3.229	1.00	2	**37,039.4**	22.520	46	6.80
32	**4823.2**	1.374	**5008.1**	1.563	2	**5972.9**	1.359	1.00	**6371.8**	1.563	1.00	2	**12,786.9**	7.403	20	3.00
33	**6856.2**	1.911	**7086.1**	2.126	2	**8427.4**	1.875	1.00	**8442.3**	2.114	1.00	2	**20,395.6**	12.494	28	4.10
34	**7817.5**	2.232	**7947.9**	2.386	2	**8596.8**	2.175	1.00	**9253.7**	2.294	1.00	2	**18,552.5**	9.881	32	5.10
35	**7929.9**	2.252	**8059.7**	2.437	2	**8813.7**	2.247	1.00	**9483.7**	2.331	1.00	2	**18,826.4**	9.480	32	5.20
36	**4954.4**	1.421	**5093.6**	1.618	2	**6219**	1.320	1.00	**6250.7**	1.500	1.00	2	**11,615.9**	6.032	30	3.30

Table 9 (continued)

Cases	PV-Grid		PV–BBS-Grid			PV–WT-Grid			PV–BBS–WT-Grid			PV–BBS–DS		
	NPC ($)	PV (kW)	NPC ($)	PV (kW)	BBS (1kWh)	NPC ($)	PV (kW)	TW	NPC ($)	PV (kW)	TW	BBS (1kWh)	NPC ($)	PV (kW)	BBS (1kWh)	DS (kW)
37	**5168.7**	1.488	**5353.6**	1.693	2	**5249.1**	1.471	1.00	**6720.6**	1.600	1.00	2	**13,357.7**	7.2153	22	3.20

contrast the PV–WT-grid configuration for cases: 2, 10, 24 and 37. These last cases are characterized by being located in the northern Amazon and Andes of Peru, which have great wind potential. Finally, there is the PV–BBS–WT-Grid configuration for all cases.

Scenario 1: demand only grid-connected

This is the traditional configuration of a rural electrification scheme; therefore, the value of the NPC mainly depends on the price of the electricity tariff. In that sense, the values obtained for each case are shown in Fig. 10.

Scenario 2: MG grid-connected without grid sellback price

Figure 11 shows the mapping of NPC and COE for each case study. The central-southern areas of the Coast and Andes regions of Peru have the lowest NPC and COE values. Particularly, the cases 23 and 30 corresponding to the villages of Rosapata and Yauli have the lowest values of NPC with $3834 and $2787, respectively; this is due to the presence of a higher solar potential in these areas. On the other hand, in the central-northern areas and the Andes and Amazon regions of Peru, higher values of NPC and COE are observed. Cases 19 and 31 corresponding to the Caballococha and Puerto Bermudez villages show the highest values of NPC with $12,070 and $11,796.07, respectively; this coincides with the lower share of solar potential in these regions. Regarding the PV–BBS-Grid, PV–WT-Grid and PV–BBS–WT-Grid hybrid system, the lowest NPC is $2977.2, $3476.6 and $4306.4, and the highest NPC is $12,282.3, $12,979.2 and $13,668.9, respectively. The difference between the NPC values of the PV-Grid and other system configurations is not significantly high, and this implies that hybrid system may still be considered economically feasible.

Regarding Fig. 11b, it can be appreciated that the COE value fluctuates between $0.063 and $0.074, which represents a decrease of 40.5% and 30.12% of the electricity tariff (0.106 $/kWh). On the other hand, the percentage of renewable energy (RE) of the grid-connected system corresponding to the PV-Grid configuration presents the maximum value of 40.6% in the case study of Nazca Rural in the central coast of Peru. On the other hand, the minimum value of 28.7% corresponds to the Nuevo Seasme case study located in the northern Amazon. Figure 12 shows the average monthly percentage of electricity from photovoltaic sources for the PV grid-connected system. The highest percentages are found in the Coast and Andes regions of Peru, while the lowest percentages are found in the Amazon region. The highest participation of renewable energy is presented in case studies 23 and 30 with a percentage of around 40%. In contrast,

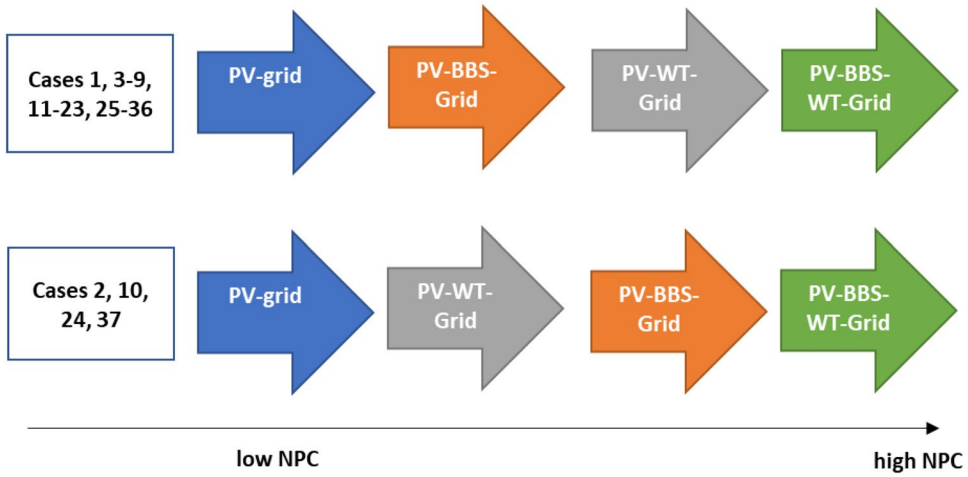

Fig. 9 NPC for all MG configurations

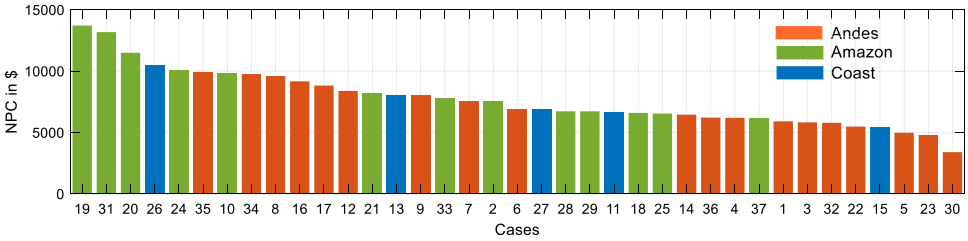

Fig. 10 NPC for all cases

with case studies 19 and 31, which present a participation of around 20% as shown in Fig. 12.

Scenario 3: MG grid-connected with grid sellback price

Through a sensitivity analysis of the simulations of all the case studies, the values of NPC and the COE of all the models are extracted. The variation of NPC values in descending order and differentiated by region is shown in Fig. 13. In all cases, combinations of photovoltaic with grid (PV-Grid) are the most optimal solutions. The locations with minimum and maximum NPC values follow the same trend as the previous case, and the highest number of cases with the lowest NPC belongs to the Andes region, while the highest PCN values belong to the Amazon region. Moreover, the COE value decreased in its average value fluctuating from $0.04 to $0.062, which represents a decrease of 60.26% and 41.5% of the electricity tariff (0.106 $/kWh).

With regard to the percentage of renewable energy, it has a similar characteristic to the previous case as show in Fig. 14. The village of Seasme has the lowest percentage of renewable energy with 36.32%, while the village of Aquispata has the highest percentage of renewable energy produced with 68.9%. It is evident that the production of renewable energy is increased in all cases, since it takes advantage of the excess generation of the PV system in hours of maximum radiation and exports it to the network, which also provides an economic revenue.

A key analysis is the energy produced in this scenario; therefore, the purchase and sale of energy are considered. Currently, the grid sellback price is an uncertain variable in Peru, which creates difficulties for the designer of the MG system. However, a price value of 30% of the grid power price value was considered by means of a sensitivity analysis. It should be noted that this value is referential. In this regard, the purchase and sale of energy were calculated for each case study as shown in Fig. 15. The maximum energy purchased corresponds to the Caballococha village (case 19) with 8252 kWh. For this same case study, a sold energy of 1643 kWh is obtained. The minimum purchased energy corresponds to the Yauli, Junin village (case 30) with 1801 kWh and a sold energy of 1202 kWh. On the other hand, the maximum energy sold corresponds to the village of Chuquibamba (case 17) with 5318 kWh. For this same case study, a purchased energy of 4413 kWh is obtained. The minimum energy sold corresponds to the Nuevo Seasme village (case 18) with 522 kWh and a purchased energy of 4159 kWh.

The net energy purchase is determined for each case according to Eq. (11) and is shown in Fig. 16. Cases 19 and 31 present the highest values of energy purchase with 6608 kWh and 7014 kWh, respectively. In addition, it is observed that in some cases, the net energy is negative, and this implies the high participation of PV energy sources

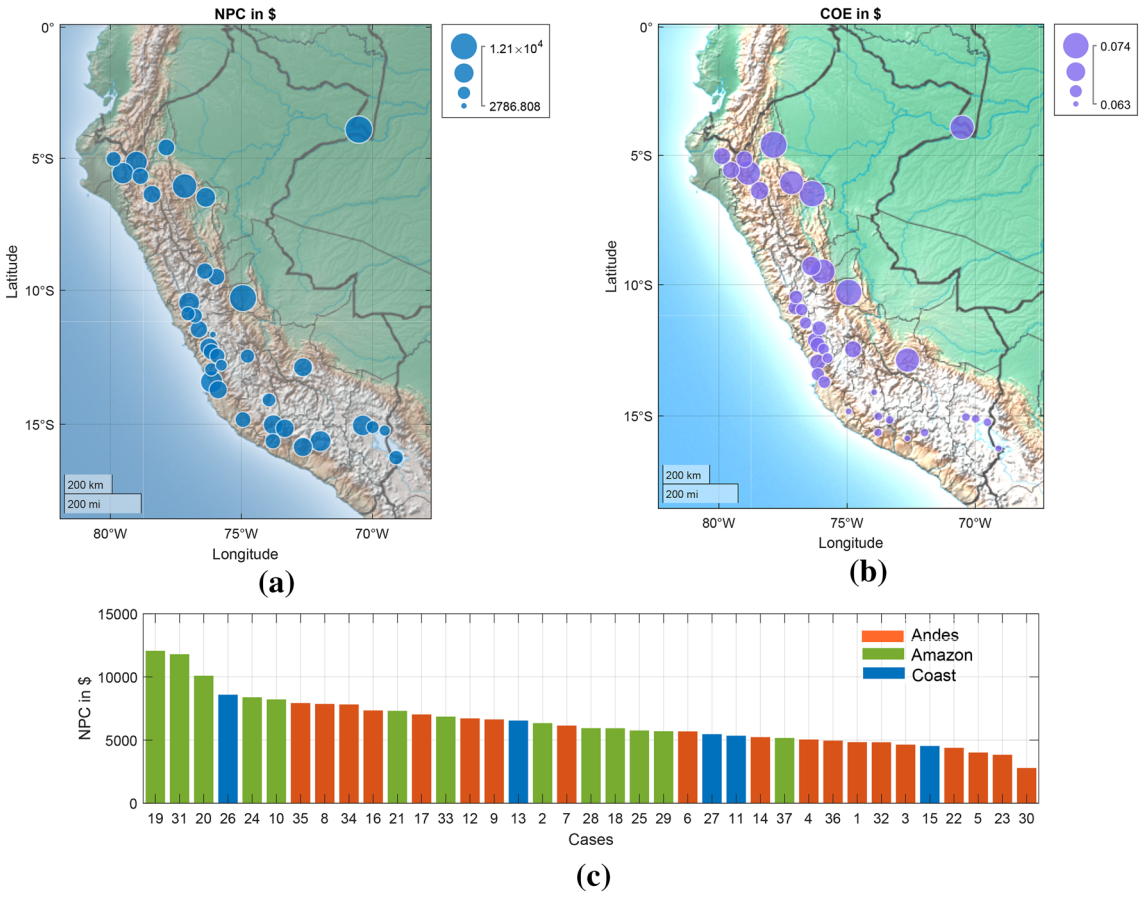

Fig. 11 MG system characteristics. **a** NPC mapping, **b** COE mapping and **c** descending order of NPC

due to the low cost and great intensity of solar irradiation. This means that these villages, apart from supplying energy to their local loads, can also supply energy to the electric network.

Scenario 4: off-grid MG system

Based on simulations, the best configuration of a stand-alone system for each case study is PV–BBS–DS except for case 3, which only requires a PV–BBS system. In this scenario, both the NPC and the COE increase compared to the grid-connected system as shown in Fig. 17.

The cases 3 and 30 have the lower NPC with $9027.0 and $7160.6, respectively. In contrast, cases 19 and 31 present higher NPC with $35,255.0 and $37,039.4, respectively. It should be noted that the latter cases correspond to the Amazon region. Therefore, it is very important to take into account this scenario because there are many villages that have disconnections from the grid for long periods of time, and this implies that the MG should also operate as an autonomous system.

With respect to the renewable energy fractions, the results showed a margin of 93.5 to 100%, and in this scenario, the lowest possible participation of diesel generators is obtained; in addition, it is highlighted that case study 3, corresponding to the Asquipata village, presents a percentage of 100% of renewable energy sources.

Scenario 5: off-grid load only with diesel generator

This configuration is based primarily on an off-grid system as it has no access to the power grid or has prolonged periods of power interruption. The value of the NPC is based primarily on the cost of fuel and is shown in Fig. 18; moreover, the value of the COE fluctuates between $1 and $1.1, which represents an increase in energy cost of 881%, making this configuration unfeasible.

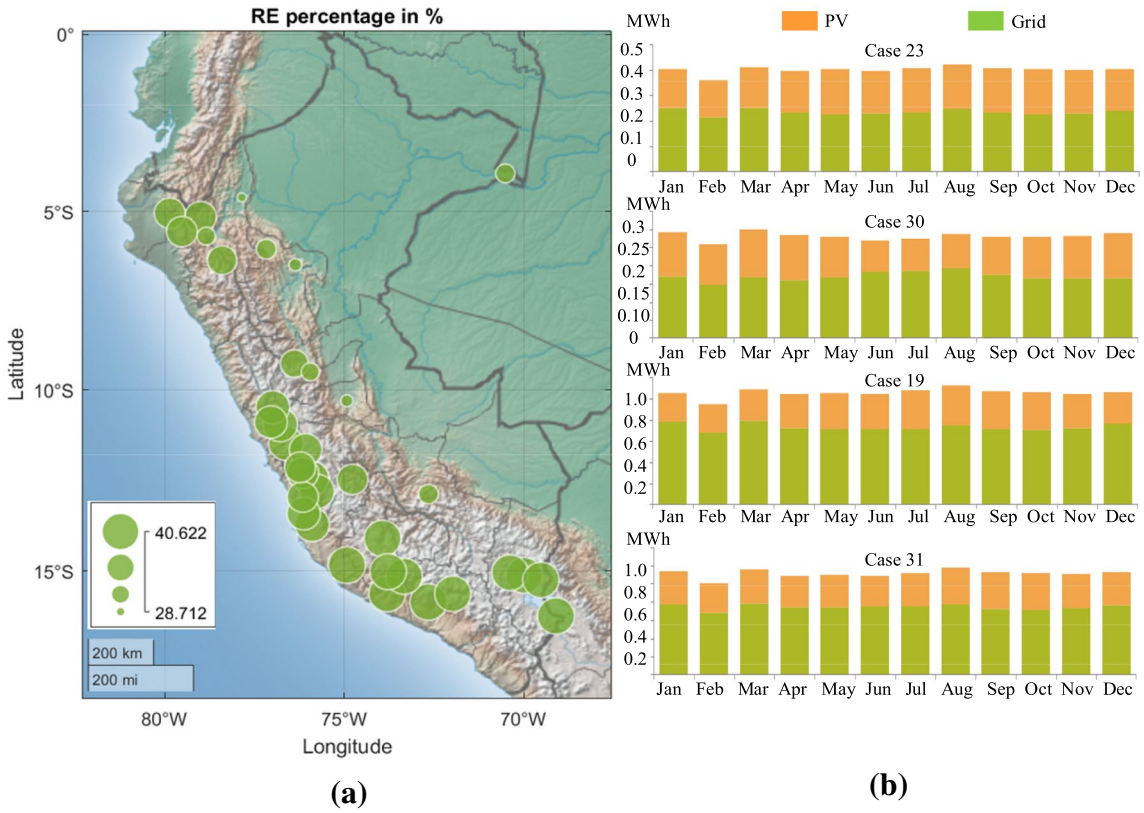

Fig. 12 Percentage of renewable energy in the PV-grid system. **a** RE percentage mapping, **b** PV and grid energy for particular cases

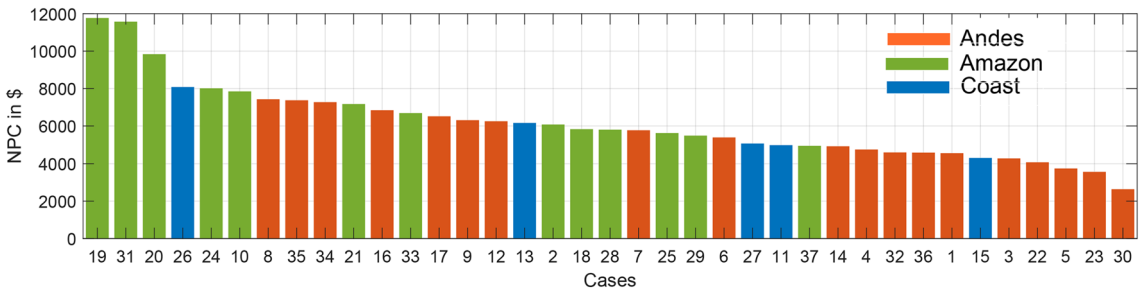

Fig. 13 NPC results of all cases for a grid-connected MG with grid sellback price

Environmental impact results

This analysis includes the emissions of carbon dioxide. Fig. 19 shows the result of total emissions for all cases. In this sense, the scenarios that include the MG system (Scenarios 2, 3 and 4) are compared with the worst-case scenario (scenario 5), which considers only diesel generators. Therefore, the average reduction in scenario 2 is 73.77%; in scenario 3, it is 76.65%, and in scenario 4, it is 97.2%. In particular, in scenario 2, the maximum reduction is 75.54% and corresponds to case 16 (Coracora), which corresponds to the southern zone of Peru, and the minimum reduction is 70.88% which corresponds to case 18 (Nuevo Seasme), located in the Amazon. In scenario 3, the maximum reduction is 75.54% corresponding to case 16, and the minimum reduction is 72.54% corresponding to case 18. In scenario 4, the maximum reduction is 100% and corresponds to case 3 (Asquipata) corresponding to an Andean zone of Peru, and the minimum reduction is 94.75% and corresponds to case 31 (Puerto Bermudez).

Economic benefit results

The annual energy charge is determined using Eq. (12), and the results are shown in Fig. 20. Cases 31 and 19 corresponding to the villages of Puerto Bermudez and Caballococha,

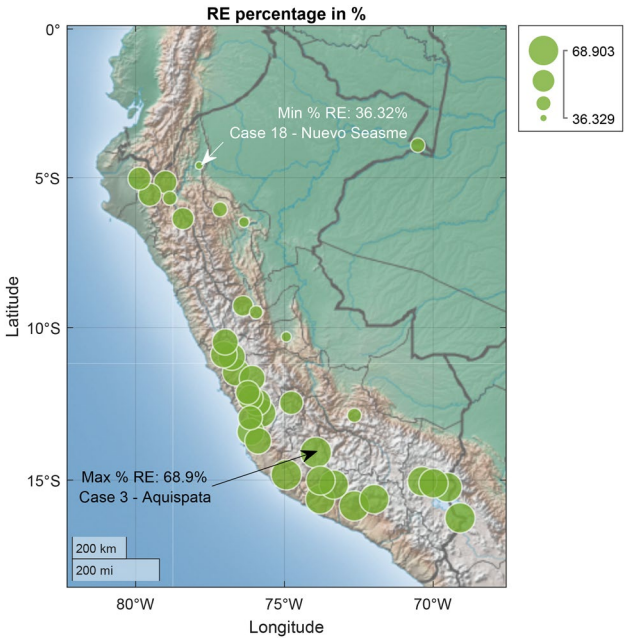

Fig. 14 Percentage of renewable energy of all cases on the map of Peru

both are located in the Amazon region of Peru, show high energy charges. In contrast, low energy charges are presented in case studies 3, 23 and 30, and these cases correspond to the Andes and Coast regions, respectively. For the grid-connected scenarios, it is evident that the high energy charges are presented with demand only grid-connected (scenario 1), and this is reduced with the inclusion of a MG system (scenario 2) and then, further reduced with the inclusion of energy market (scenario 3). With respect to the stand-alone system, it can be seen that the energy charge falls radically; while in the case of only diesel generator (scenario 5), the charges are around $2000 and $5000; in the cases with MG system, the charges are less than $450.

The annual savings in electric utility bills are shown in Fig. 21, and this analysis is carried out by comparing two scenarios. The first comparison, under current conditions, is the grid-connected MG system with the loads only connected to the grid (Fig. 21a). In this context, the greatest benefits correspond to case 19 (Caballococha) located in the Amazon region and case 27 (Nazca Rural) located in the central coast of Peru, and the annual savings are $363.4 and $398.2, respectively.

The second comparison, for future conditions of the electrical networks, is the grid-connected MG system with and without grid sellback price (Fig. 21b). In this regard, the greatest benefits correspond to case studies 34 (Pucara) and 35 (Valle del Colca) both in the south-Andes of Peru, and the annual savings are $248.6 and $252, respectively.

The third comparison, under current conditions, is the off-grid MG system with off-grid load only with diesel generator (Fig. 21c). In this respect, the greatest benefits

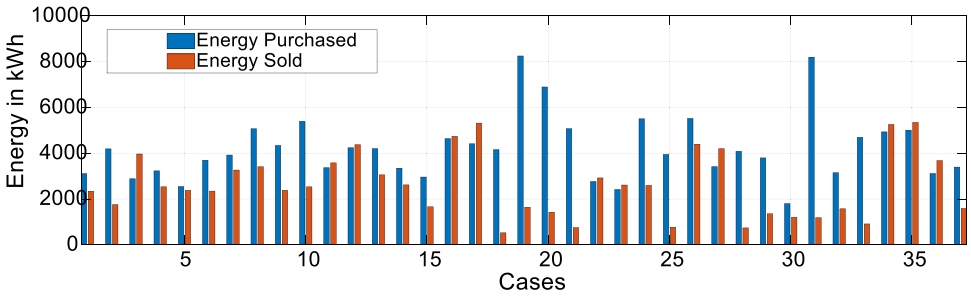

Fig. 15 Energy purchased and sold

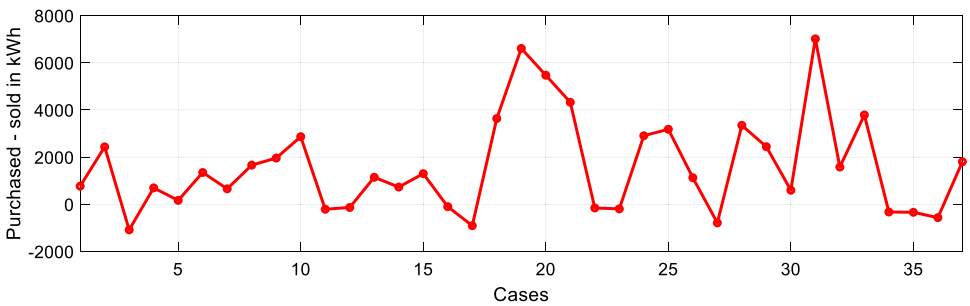

Fig. 16 Net energy purchase for all cases

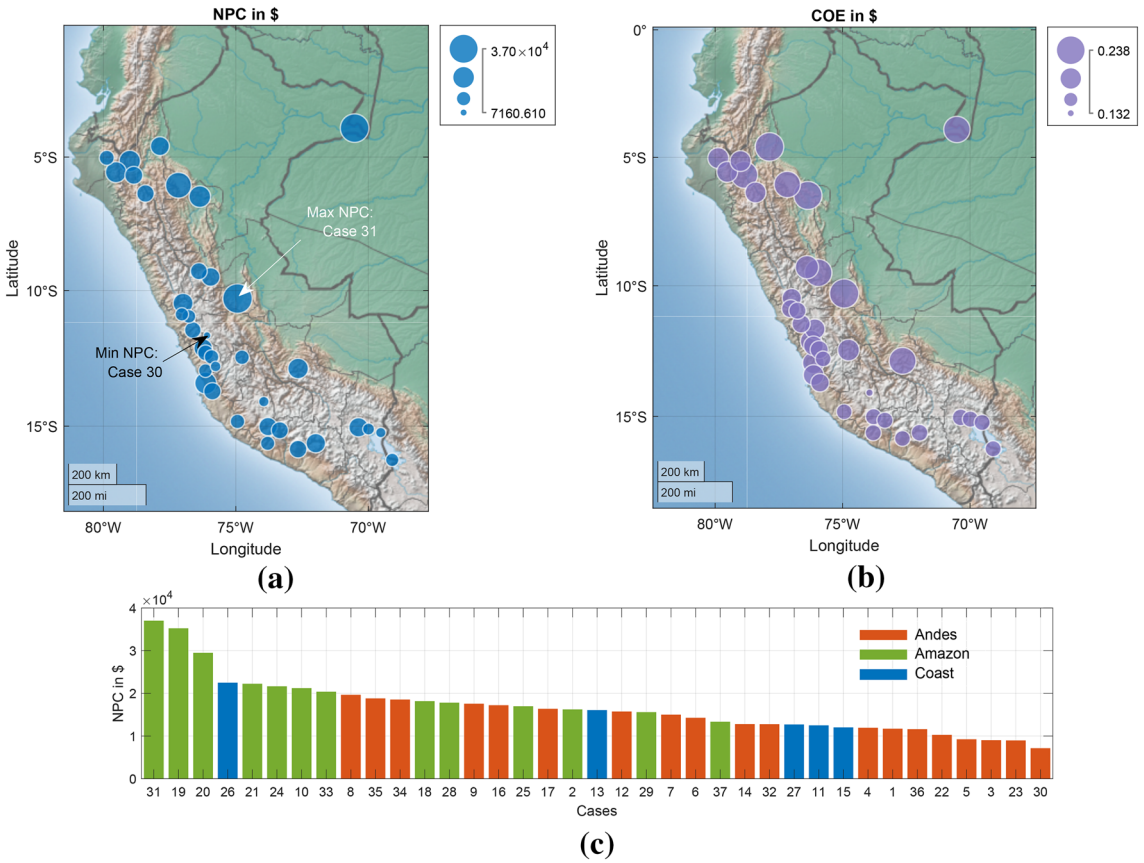

Fig. 17 PV–BBS–DS system characteristics. **a** NPC mapping, **b** COE mapping and **c** descending order of NPC

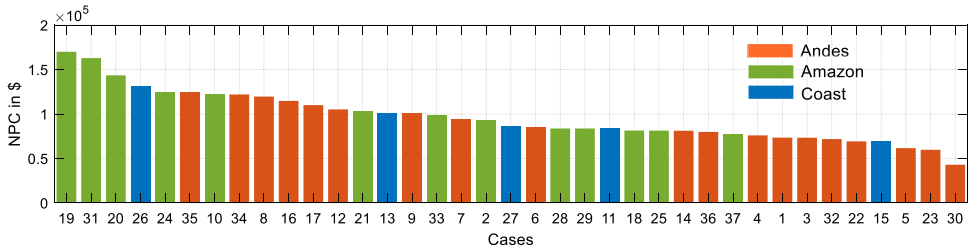

Fig. 18 NPC results of all cases for off-grid load only with diesel generator

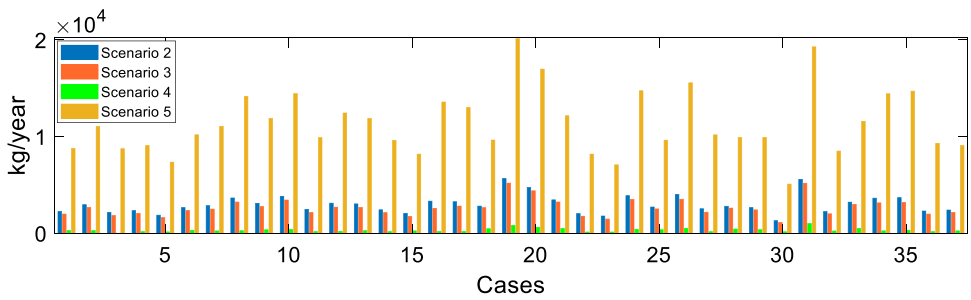

Fig. 19 Emissions for all case studies

correspond to case studies 19 (Caballococha) and 31 (Puerto bermudez) both in the Amazon region of Peru, and the annual savings are $4976 and $4668, respectively.

Finally, Fig. 22 shows the mapping of the economic benefits for all cases, where the areas with the greatest economic potential for microgrids facility are clearly

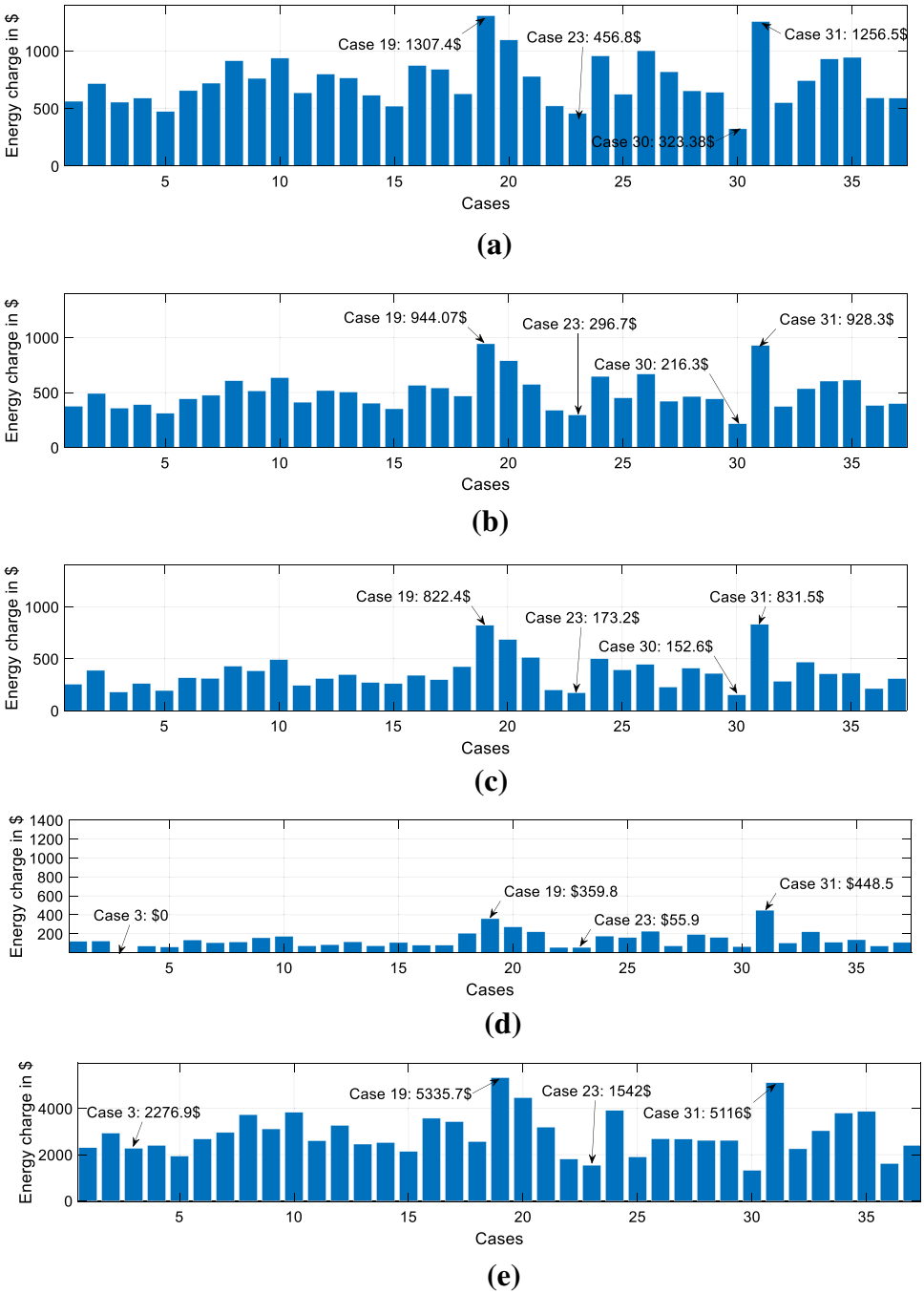

Fig. 20 Energy charge for all cases. **a** Scenario 1, **b** scenario 2, **c** scenario 3, **d** scenario 4 and **e** scenario 5

observed. Under current conditions, grid-connected, and with the purpose of installing MGs in rural areas, the highest utilities correspond to the coast and Andes of southern Peru (Fig. 22a and b). In addition, under stand-alone MG conditions, the best utilities are found in the Amazon region of Peru (Fig. 22c).

Conclusion

According to the features of the costs associated with an MG, geographic location, and load characteristics, this work determines the optimal configuration of an MG at the minimum investment cost for rural areas of Peru. The results obtained show that the NPC values, which is the difference between the present value of the future income that will be received and the amount invested to carry out the project, show positive values; that is, meaning that the projects are

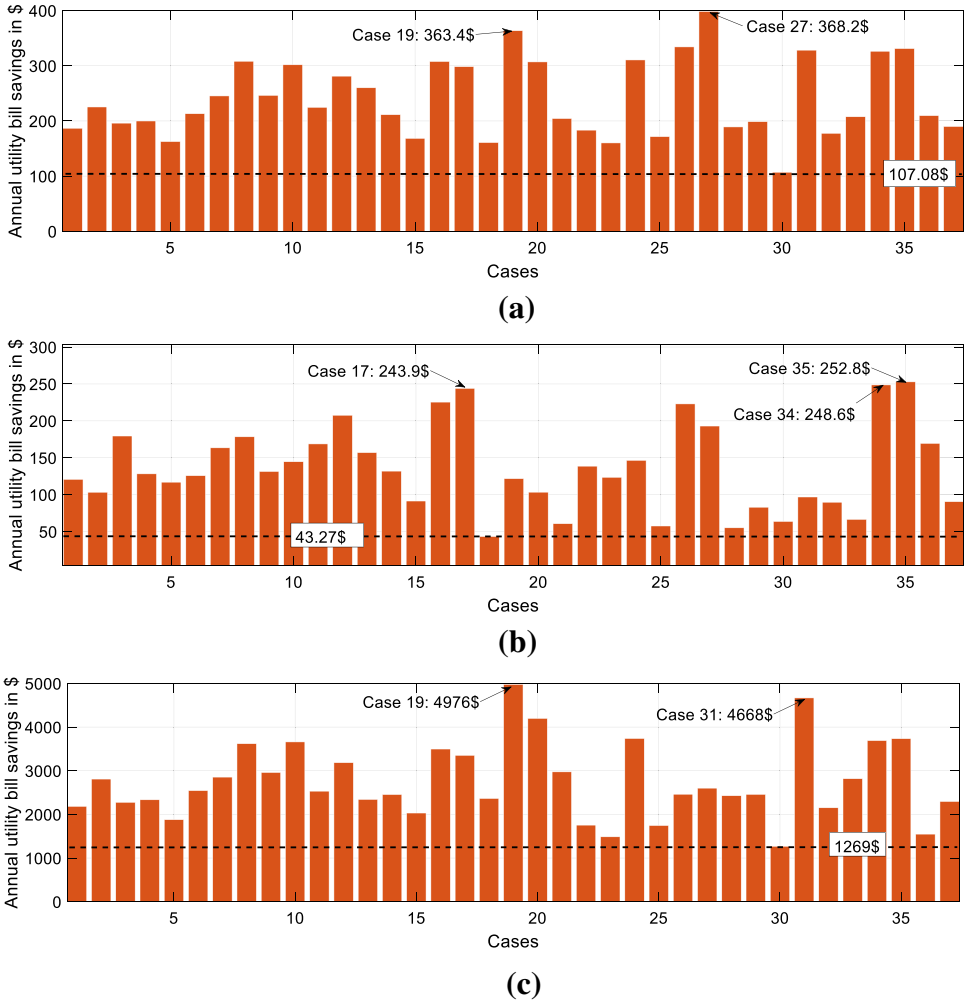

Fig. 21 Annual savings on utility bills for all cases. **a** Comparison 1, **b** Comparison 2 and **c** Comparison 3

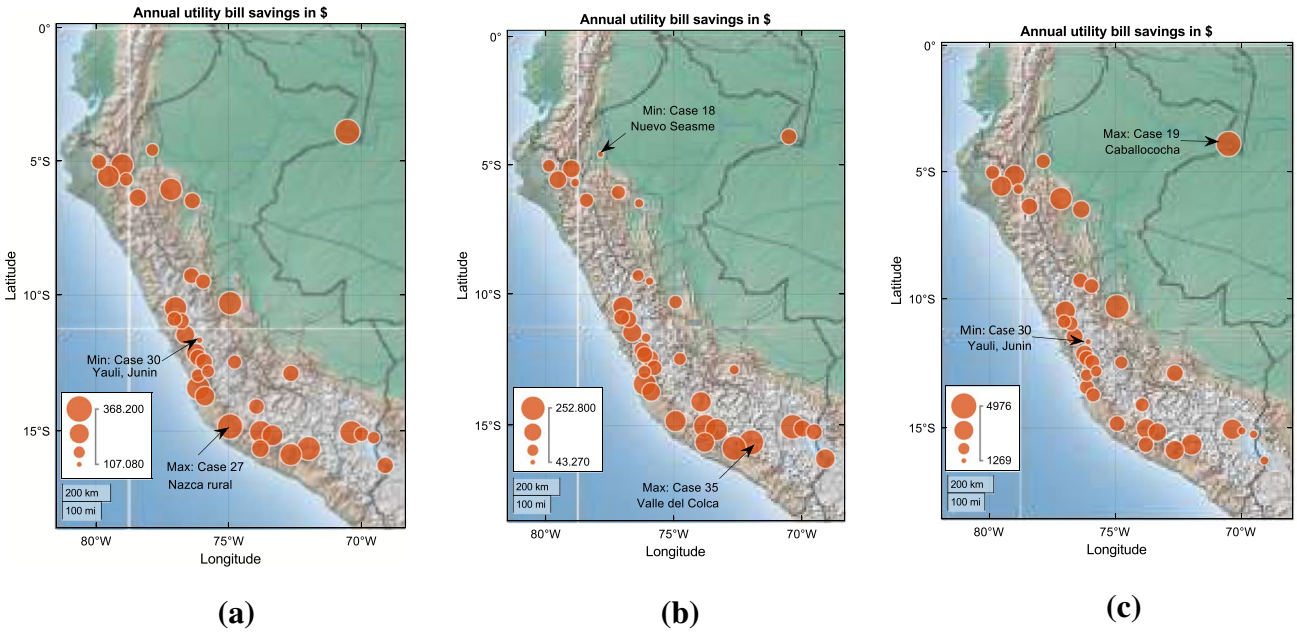

Fig. 22 Mapping of annual savings on utility bills for all cases. **a** Comparison 1, **b** Comparison 2 and **c** Comparison 3

feasible. In addition, the annual economic benefits through the use of the MG are evident for all cases. In this regard, all possible scenarios of a rural load have been considered such as demand only grid-connected, MG grid-connected without grid sellback price, MG grid-connected with grid sellback price, off-grid MG system, and off-grid load only with diesel generator. Therefore, the scenarios grid-connected converge in the optimal configuration for each case study of PV-Grid type; however, there is no great variation with the PV–BBS-Grid and PV–WT-Grid of hybrid configurations, which are also economical solutions. Whereas, off-grid scenarios verify that the optimal configuration includes the PV, battery system and diesel generator. On the other hand, the inclusion of the grid sellback price has verified the increase in economic benefits, which is an attractive investment for the upcoming market models. With respect to the environmental impact, all cases have shown a considerable reduction, mainly compared to a system with only diesel generators, the results revealed that the average reduction ranges from 73.77 to 97.2%, which makes these projects very sustainable.

Consequently, the analysis of the scenarios indicates that better benefits of the demands connected to the grid, with the implementation of the MGs, are mainly located in the coastal and Andean regions of Peru with greater participation in the southern zone. The results show savings from $107.08 to $368.2 per year for a condition without energy sales; however, these savings increase further by $43.27 to $252.8 with the inclusion of energy market. On the other hand, this analysis also indicates that the greatest benefits for stand-alone demands are found in the Amazon region of Peru, leaving the Andean areas in second place. The results show savings from $1269 to $4976 per year. Finally, a tool was presented that allows the mapping of parameters such as NPC, COE, percentage of renewable, emissions, energy and annual utility in a specific study area; therefore, this can be used to verify potential locations for installing a MG in any geographic area. As a result, this work could be considered as reference models for the development of future implementation of MG projects.

Acknowledgements Not applicable.

Author contributions Conceptualization, JCQ and FJA; methodology, JCQ; software, JCQ; validation, JCQ, FJA and AEO; formal analysis, JCQ, AEO and FJA; resources, JCQ; writing—original draft preparation, JCQ, AEO, FJA; writing - review and editing, JCQ, AEO, FJA; visualization, JCQ, AEO, FJA; project administration, JCQ. All authors have read and agreed to the published version of the manuscript.

Funding This work was supported by Universidad Tecnológica del Perú.

Data availability Enquiries about data availability should be directed to the authors.

Declarations

Competing interests The authors declare no competing interests.

References

Adefarati T, Obikoya GD (2019) Techno-economic evaluation of a grid-connected microgrid system. Int J Green Energy 16(15):1497–1517. https://doi.org/10.1080/15435075.2019.1671421

ADINELSA (2022) Pliego Tarifario. http://www.adinelsa.com.pe/adinelsaweb/index.php/atencion-al-cliente/tarifas

Aemro YB, Moura P, De Almeida AT (2020) Design and modeling of a standalone DC-microgrid for off-grid schools in rural areas of developing countries. Energies 13(23):6379. https://doi.org/10.3390/EN13236379

Ajlan A, Tan CW, Abdilahi AM (2017) Assessment of environmental and economic perspectives for renewable-based hybrid power system in Yemen. Renew Sustain Energy Rev 75:559–570. https://doi.org/10.1016/J.RSER.2016.11.024

Al-Ammar EA, Habib HUR, Kotb KM, Wang S, Ko W, Elmorshedy MF, Waqar A (2020) Residential community load management based on optimal design of standalone HRES with model predictive control. IEEE Access 8:12542–12572. https://doi.org/10.1109/ACCESS.2020.2965250

Arnold GW (2011) Challenges and opportunities in smart grid: a position article. Proc IEEE 99(6):922–927. https://doi.org/10.1109/JPROC.2011.2125930

Aziz MS, Khan MA, Khan A, Nawaz F, Imran M, Siddique A (2020) Rural electrification through an optimized off-grid microgrid based on biogas solar and hydro power. In 2020 International conference on engineering and emerging technologies, ICEET 2020. https://doi.org/10.1109/ICEET48479.2020.9048222

Berizzi A, Delfanti M, Falabretti D, Mandelli S, Merlo M (2019) Electrification processes in developing countries: grid expansion, microgrids, and regulatory framework. Proc IEEE 107(9):1981–1994. https://doi.org/10.1109/JPROC.2019.2934866

Byrne RH, Nguyen TA, Copp DA, Chalamala BR, Gyuk I (2017) Energy management and optimization methods for grid energy storage systems. IEEE Access 6:13231–13260. https://doi.org/10.1109/ACCESS.2017.2741578

Catuogno G, Torres L, Proietti L, Garcia G (2019) Methodology for the selection and sizing of an isolated microgrid based on economic criteria. IEEE Latin Am Trans 17(11):1761–1770. https://doi.org/10.1109/TLA.2019.8986413

Fraunhofer (2021) Recent facts about photovoltaics in Germany. https://www.ise.fraunhofer.de/en/publications/studies/recent-facts-about-pv-in-germany.html

Gabr AZ, Helal AA, Abbasy NH (2021) Multiobjective optimization of photo voltaic battery system sizing for grid-connected residential prosumers under time-of-use tariff structures. IEEE Access 9:74977–74988. https://doi.org/10.1109/ACCESS.2021.3081395

Hernandez L (2019) Microrredes eléctricas: Integración de generación renovable distribuida, almacenamiento distribuido e inteligencia, vol 558. Ibergarceta Publicaciones S.L. (eds), Madrid

Homer (2022) HOMER pro. https://www.homerenergy.com/products/pro/docs/latest/index.html

Hossain M, Mekhilef S, Olatomiwa L (2017) Performance evaluation of a stand-alone PV-wind-diesel-battery hybrid system feasible for a large resort Center in South China Sea, Malaysia. Sustain Cities Soc 28:358–366. https://doi.org/10.1016/J.SCS.2016.10.008

Imfeld N, Sedlmeier K, Gubler S, Correa Marrou K, Davila CP, Huerta A, Lavado-Casimiro W, Rohrer M, Scherrer SC, Schwierz C (2021) A combined view on precipitation and temperature climatology and trends in the southern Andes of Peru. Int J Climatol 41(1):679–698. https://doi.org/10.1002/JOC.6645

INEI (2019) Instituto Nacional de Estadistica e Informatica. https://m.inei.gob.pe/estadisticas/indice-tematico/poblacion-y-vivienda/

Islam MS, Akhter R, Rahman MA (2018) A thorough investigation on hybrid application of biomass gasifier and PV resources to meet energy needs for a northern rural off-grid region of Bangladesh: a potential solution to replicate in rural off-grid areas or not? Energy 145:338–355. https://doi.org/10.1016/J.ENERGY.2017.12.125

Jha SK, Stoa P, Uhlen K (2017) Green and hybrid microgrid for rural electrification.In IEEE region 10 humanitarian technology conference 2016, R10-HTC 2016—proceedings. https://doi.org/10.1109/R10-HTC.2016.7906841

Jin S, Kim H, Kim TH, Shin H, Kwag K, Kim W (2019) A study on designing off-grid system using HOMER pro—a case study. In IEEE international conference on industrial engineering and engineering management, 2019-December, pp 1851–1855. https://doi.org/10.1109/IEEM.2018.8607423

Khare V, Nema S, Baredar P (2016) Optimization of hydrogen based hybrid renewable energy system using HOMER, BB-BC and GAMBIT. Int J Hydrogen Energy 41(38):16743–16751. https://doi.org/10.1016/J.IJHYDENE.2016.06.228

Kroposki B, Bernstein A, King J, Vaidhynathan D, Zhou X, Chang CY, Dallanese E (2020) Autonomous energy grids: controlling the future grid with large amounts of distributed energy resources. IEEE Power Energy Mag 18(6):37–46. https://doi.org/10.1109/MPE.2020.3014540

Kumar A, Singh AR, Deng Y, He X, Kumar P, Bansal RC (2018) A novel methodological framework for the design of sustainable rural microgrid for developing nations. IEEE Access 6:24925–24951. https://doi.org/10.1109/ACCESS.2018.2832460

Lasseter RH (2011) Smart distribution: coupled microgrids. Proc IEEE 99(6):1074–1082. https://doi.org/10.1109/JPROC.2011.2114630

Liu G, Rasul MG, Amanullah MTO, Khan MMK (2012) Techno-economic simulation and optimization of residential grid-connected PV system for the Queensland climate. Renew Energy 45:146–155. https://doi.org/10.1016/J.RENENE.2012.02.029

MEM (2011) Guía Simplificada para la Identificación, Formulación y Evaluación Social de Proyectos deElectrificación Rural, a Nivel de Perfil. Ministerio de Economía y Finanzas. https://fdocuments.es/document/diseno-electrificacion-rural-corregido.html

Mojumder MRH, Hasanuzzaman M, Cuce E (2022) Prospects and challenges of renewable energy-based microgrid system in Bangladesh: a comprehensive review. Clean Technol Environ Policy. https://doi.org/10.1007/S10098-022-02301-5

Mustafa Kamal M, Asharaf I, Fernandez E (2022) Optimal renewable integrated rural energy planning for sustainable energy development. Sustain Energy Technol Assess. https://doi.org/10.1016/J.SETA.2022.102581

Najafi B, Najafi H, Idalik MD (2011) Computational fluid dynamics investigation and multi-objective optimization of an engine air-cooling system using genetic algorithm. J Mech Eng Sci 225(6):1389–1398. https://doi.org/10.1177/0954406210395877

NASA (2022) NASA POWER. Prediction of worldwide energy resources. https://power.larc.nasa.gov/

Nnaji EC, Adgidzi D, Dioha MO, Ewim DRE, Huan Z (2019) Modelling and management of smart microgrid for rural electrification in sub-saharan Africa: the case of Nigeria. Electr J. https://doi.org/10.1016/J.TEJ.2019.106672

Nurunnabi M, Roy NK, Hossain E, Pota HR (2019) Size optimization and sensitivity analysis of hybrid wind/PV micro-grids—a case study for Bangladesh. IEEE Access 7:150120–150140. https://doi.org/10.1109/ACCESS.2019.2945937

Ozerdem B, Ozer S, Tosun M (2006) Feasibility study of wind farms: a case study for Izmir, Turkey. J Wind Eng Ind Aerodyn 94(10):725–743. https://doi.org/10.1016/J.JWEIA.2006.02.004

Rafi MAA, Jaman MSK, Hasan MN, Islam MR, Mahmud MAP, Kouzani AZ, Al NA (2021) Renewable energy-based hybrid microgrid for economically effective coastal electrification. IEEE Trans Appl Supercond. https://doi.org/10.1109/TASC.2021.3089118

Ray A, Jana K, Assadi M, De S (2018) Distributed polygeneration using local resources for an Indian village: multiobjective optimization using metaheuristic algorithm. Clean Technol Environ Policy 20(6):1323–1341. https://doi.org/10.1007/S10098-018-1562-Y/FIGURES/9

Sinha S, Chandel SS (2015) Review of recent trends in optimization techniques for solar photovoltaic–wind based hybrid energy systems. Renew Sustain Energy Rev 50:755–769. https://doi.org/10.1016/J.RSER.2015.05.040

Suresh V, Muralidhar M, Kiranmayi R (2017) Optimization of hybrid renewable energy systems for sustainable and economical power supply at SVCET Chittoor. I-Manag J Power Syst Eng. 5(1):26. https://doi.org/10.26634/JPS.5.1.13534

Wang D, Ge S, Jia H, Wang C, Zhou Y, Lu N, Kong X (2014) A demand response and battery storage coordination algorithm for providing microgrid tie-line smoothing services. IEEE Trans Sustain Energy 5(2):476–486. https://doi.org/10.1109/TSTE.2013.2293772

Zahboune H, Zouggar S, Krajacic G, Varbanov PS, Elhafyani M, Ziani E (2016) Optimal hybrid renewable energy design in autonomous system using modified electric system cascade analysis and homer software. Energy Convers Manage 126:909–922. https://doi.org/10.1016/J.ENCONMAN.2016.08.061

Zhao J. (2020). Research on optimized configuration of microgrid with distributed energy in commercial users in hainan province. In: IOP conference series: earth and environmental science, vol 461, no 1. https://doi.org/10.1088/1755-1315/461/1/012057